



Universidad Autónoma
de Madrid

Biblos-e Archivo
Repositorio Institucional UAM

Repositorio Institucional de la Universidad Autónoma de Madrid

<https://repositorio.uam.es>

Esta es la **versión de autor** del artículo publicado en:

This is an **author produced version** of a paper published in:

Cell Metabolism 14.6 (2011): 768-779

DOI: <https://doi.org/10.1016/j.cmet.2011.10.008>

Copyright: © 2011 Elsevier Inc. This manuscript version is made available under the CC-BY-NC-ND 4.0 licence <http://creativecommons.org/licenses/by-nc-nd/4.0/>

El acceso a la versión del editor puede requerir la suscripción del recurso

Access to the published version may require subscription

Induction of the mitochondrial NDUFA4L2 protein by HIF-1 α decreases oxygen consumption by inhibiting Complex I activity

Daniel Tello^{1*}, Eduardo Balsa^{1*}, Bárbara Acosta-Iborra¹, Esther Fuertes-Yebra¹, Ainara Elorza¹, Ángel Ordóñez¹, María Corral-Escariz¹, Inés Soro¹, Elia López-Bernardo¹, Ester Perales-Clemente², Antonio Martínez-Ruiz¹, José Antonio Enríquez^{2,3}, Julián Aragonés¹, Susana Cadenas^{1,4} and Manuel O. Landázuri¹

¹Servicio de Inmunología, Hospital Universitario de La Princesa, Universidad Autónoma de Madrid, Instituto de Investigación Sanitaria Princesa (IIS-IP), Madrid, 28006, Spain

²Centro Nacional de Investigaciones Cardiovasculares Carlos III (CNIC), Madrid, 28029, Spain

³Departamento de Bioquímica y Biología Molecular y Celular, Facultad de Ciencias, Universidad de Zaragoza, 50013, Spain

⁴Departamento de Biología Molecular, Facultad de Ciencias, Universidad Autónoma de Madrid, Madrid, 28049, Spain

Correspondence: mortiz.hlpr@salud.madrid.org

*D.T. and E.B. contributed equally to this work.

Summary

The fine regulation of mitochondrial function has proved to be an essential metabolic adaptation to fluctuations in oxygen availability. During hypoxia, cells activate an anaerobic switch that favors glycolysis and attenuates the mitochondrial activity. This switch involves the hypoxia-inducible transcription factor-1 (HIF-1). We have identified a HIF-1 target gene, the mitochondrial NDUFA4L2 (NADH dehydrogenase (ubiquinone) 1 alpha subcomplex, 4-like 2). Our results, obtained employing NDUFA4L2-silenced cells and NDUFA4L2 knockout murine embryonic fibroblasts, indicate that hypoxia-induced NDUFA4L2 attenuates mitochondrial oxygen consumption involving inhibition of Complex I activity, which limits the intracellular ROS production under low oxygen conditions. Thus, reducing mitochondrial Complex I activity via NDUFA4L2 appears to be an essential element in the mitochondrial reprogramming induced by HIF-1.

Introduction

Aerobic organisms have developed specific systems to deliver oxygen to cells in different anatomical locations. However, insufficient oxygen supply and the ensuing hypoxia is a hallmark of different pathological situations. In response to hypoxia, cells activate a metabolic program that reduces oxygen consumption by actively lowering mitochondrial oxidative phosphorylation (OXPHOS) activity, the main oxygen-consuming process in most cell types, accompanied by an increase in glucose uptake and the rate of glycolysis

(Aragones et al., 2008; Iyer et al., 1998; Kim et al., 2006; Papandreou et al., 2006). This hypoxic adaptation is due to the expression of genes triggered by hypoxia inducible factors (HIFs) (Aragones et al., 2009). HIFs are master transcription factors regulated in an O₂-dependent manner by a family of prolyl hydroxylases (PHDs), which use O₂ as a substrate to hydroxylate HIF- α subunits in conditions of normoxia (Kaelin and Ratcliffe, 2008). These hydroxylated substrates are then ubiquitinated after recognition by VHL and they are degraded by the proteasome. By contrast, PHD activity is inhibited in hypoxic conditions and accordingly, HIF- α subunits accumulate, heterodimerize with HIF- β and activate the expression of HIF-dependent target genes (Schofield and Ratcliffe, 2004; Semenza, 2004, 2009).

Among the genes whose expression is up-regulated by HIFs are glucose transporters, like Glut1, as well as key enzymes involved in glycolysis (Iyer et al., 1998). The PDK1 and PDK3 genes that code for pyruvate dehydrogenase kinases are also up-regulated, which results in increased phosphorylation and inactivation of pyruvate dehydrogenase (PDH), the enzyme that converts pyruvate to acetyl-CoA (Kim et al., 2006; Lu et al., 2008; Papandreou et al., 2006). This process limits the substrate available for the tricarboxylic acid cycle (TCA) and thus, for OXPHOS activity. Mitochondrial respiration is also regulated by additional mechanisms that maximize respiratory efficiency under conditions of reduced O₂ availability. Genes that regulate cytochrome c oxidase (the ETC Complex IV that reduces O₂ to H₂O) are also regulated by HIFs, including COX4-2 isoform and the LON protease, which produces a switch from isoform COX4-1 to COX4-2 that optimizes the efficiency of respiration under hypoxic conditions (Fukuda et al., 2007).

Complex I (NADH:ubiquinone oxidoreductase) is the largest and least understood component of the respiratory chain. This Complex catalyzes the first step in the electron transport chain (ETC), transferring electrons from NADH to a non-covalently bound flavin mononucleotide (FMN) and then, via a series of iron–sulfur clusters (FeS), to the final ubiquinone acceptor. Complex I consists of 45 different subunits that are assembled into a structure of ~1 MDa, and while 7 subunits are encoded by mitochondrial DNA, the remaining 38 are coded for by the nuclear genome (Carroll et al., 2006). The activity of the Complex I is affected by hypoxia, either through post-translational modification (Frost et al., 2005) or the reduced expression of mitochondrial genes (Chan et al., 2009). Here we report that HIF-1 induces the expression of the NADH dehydrogenase (ubiquinone) 1 alpha subcomplex subunit 4-like 2 gene (NDUFA4L2: also called NADH-ubiquinone oxidoreductase MLRQ subunit homologue -NUOMS), catalogued as a component of ETC Complex I due to its high sequence identity with NDUFA4. It was previously described using mRNA array technology that NDUFA4L2 is over-expressed in VHL-deficient cell lines and tumors (Favier et al., 2009; Papandreou et al., 2006), as well as in neuroblastoma cells in hypoxia (Fredlund et al., 2008) and in pathological conditions like rheumatoid arthritis (Andreas et al., 2009). Although the physiological function of this protein remains unclear, we show here that it is involved in lowering mitochondrial oxygen consumption and Complex I activity, thereby reducing ROS production. This provides a point in the regulation of mitochondrial activity that can reprogram Complex I activity under low oxygen conditions.

Results

Hypoxia induces NDUFA4L2 expression in primary cultures and tumor cells *in vitro*, as well as *in vivo*, a protein that is localized to mitochondria

We hypothesized that, as the principal electron acceptor, Complex I could be a key regulatory point in the control of the ETC during hypoxia. To identify Complex I components that might be regulated by moderate hypoxia, we used an mRNA array to analyze the expression of genes in HeLa cells maintained for short periods of time (6 h) in 1% O₂. We detected the expression of 44 genes of Complex I in the array: 40 genes encoded by nuclear DNA, and 4 encoded in the mitochondria (ND1, ND2, ND3 and ND6). Of all these genes, only NDUFA4L2 was clearly induced by hypoxia, whereas the other genes encoded by nuclear DNA remained unchanged (Table S1). By contrast and as described previously (Piruat and Lopez-Barneo, 2005), the other mitochondrially encoded genes underwent a marked down-regulation in these hypoxic conditions (Table S1). It is important to note that NDUFA4L2 gene is strongly induced by hypoxia. In fact, it appears among the first twelve genes more induced by hypoxia in the mRNA study (Table S2).

This microarray data was validated by RT-PCR on mRNA isolated from HeLa and PC-12 cells exposed to hypoxia. Indeed, RT-PCR assays confirmed that NDUFA4L2 expression was strongly up-regulated in response to hypoxia (Figure 1A), while such conditions did not change the levels of other Complex I genes encoded in the nucleus, such as NDUFA4, NDUFAB1 or NDUFB4,

although ND1 and ND6 expression was down-regulated (Figure S1A). Up-regulation of NDUFA4L2 expression was also observed in HUVEC and cardiomyocytes subjected to hypoxia and after treatment with prolylhydroxylase inhibitors such as dimethyloxaloylglycine (DMOG) and deferroxamine (Figure 1B). The efficacy of hypoxia and DMOG in these experiments was corroborated by the marked up-regulation of previously recognized HIF target genes such as PHD3, BNIP3 and Glut 1 (Figure S1B). In addition, NDUFA4L2 expression was induced in brain tissue of mice exposed to 7.5% O₂ for 18 h (Figure 1C). An increase in NDUFA4L2 protein was also evident in response to hypoxia in different cell types and brain tissue (Figure 1D) with an antibody specific to this protein that did not recognize the homologous NDUFA4 protein (Figure S1C). Moreover, the increase in NDUFA4L2 protein induced by hypoxia was evident in cardiomyocytes when assessed by immunofluorescence (Figure 1E).

We analyzed the cellular localization of NDUFA4L2 in normoxic and hypoxic conditions. A bioinformatics approach predicted that NDUFA4L2 would be localized in mitochondria (Table S3) and this prediction was then confirmed experimentally by analyzing mitochondrial and cytoplasmic fractions from HeLa cells. NDUFA4L2 was clearly enriched in the mitochondrial fraction under hypoxic conditions (Figure 1F) and immunofluorescence showed a clear co-localization of NDUFA4L2 and cytochrome c in HL-1 cells (Figure 1G), as well as the co-localization of NDUFA4L2 and the mitochondria-selective dye MitoTracker in HeLa cells (Figure S1D). These results confirmed the mitochondrial location of NDUFA4L2.

HIF-1 α regulates NDUFA4L2 induction

To investigate whether hypoxia-induced NDUFA4L2 expression was mediated by HIF transcription factors, we first silenced HIF-1 β , the common partner of HIF-1 α and HIF-2 α , thereby impairing the canonical HIF transcriptional response. Interference of HIF-1 β expression abolished the induction of NDUFA4L2 during hypoxia (Figure 2A), as well as the response of PHD3 (included as a control of HIF-target gene; Figure S2A), indicating that HIF transcriptional activity is essential for NDUFA4L2 induction.

To study the specific role of HIF-1 α and HIF-2 α in the response of NDUFA4L2 to hypoxia, we performed RNA interference assays in human renal carcinoma RCC4 cells that constitutively stabilize HIF-1 α and HIF-2 α through the absence of VHL. Likewise, the response of NDUFA4L2 was also assessed in RCC4/VHL cells in which VHL expression was restored and hence, both HIF-1 α and HIF-2 α were exclusively up-regulated in response to hypoxia. In line with the role of HIF activity in NDUFA4L2 regulation, there was a robust up-regulation of NDUFA4L2 in hypoxic RCC4/VHL cells, whereas there was marked and constitutive NDUFA4L2 expression in normoxic RCC4 cells that was only minimally up-regulated in hypoxic conditions (Figure 2B). HIF-1 α interference abrogated the expression of NDUFA4L2 in both normoxic and hypoxic RCC4 cells (Figure 2B), as well as hypoxia-driven NDUFA4L2 expression in RCC4/VHL cells (Figure 2B). By contrast, HIF-2 α interference did not affect the expression of NDUFA4L2 in RCC4/VHL cells exposed to hypoxia, and no significant effect was observed in RCC4 cells in either normoxic or hypoxic conditions (Figure 2B). The control experiments for the interference

assays showed a specific reduction of HIF-1 α or HIF-2 α mRNA expression (Figure S2B).

We further confirmed these data in mouse embryonic fibroblasts (MEFs) from Hif1 $\alpha^{+f/+f}$ /Cre conditional mice in which HIF-1 α was lost after tamoxifen treatment. As a control, we employed tamoxifen Hif1 $\alpha^{+/+}$ /Cre MEFs that lacked the CRE recombination sites required for HIF-1 α ablation. The hypoxic induction of NDUFA4L2 expression, as well as that of the HIF target gene PHD3, were only abrogated in Hif1 $\alpha^{+f/+f}$ /Cre conditional MEFs following tamoxifen exposure, whereas they were still expressed in Hif1 $\alpha^{+/+}$ /Cre MEFs (Figure 2C and S2C). Hence, the hypoxic induction of NDUFA4L2 appeared to be mostly mediated by HIF-1 α .

To identify possible hypoxia response elements (HREs) responsible for the induction of NDUFA4L2, the proximal promoter region (intron 1) of NDUFA4L2 was analyzed identifying two putative HREs at +43 and +1344 (Figure 2D). The +43 site is highly conserved between different species, unlike the +1344 site. Chromatin immunoprecipitation (ChIP) assays were performed on HeLa cells grown under normoxic or hypoxic conditions, and after treatment with DMOG. To evaluate HIF-1 α binding to NDUFA4L2 regulatory sequences, quantitative-PCR was performed using specific primers for the putative HRE site (A), the non-conserved HRE site (B), and a negative site (C). ChIP assays for PDK1, a well-known HIF-1 α target, were also performed as a positive control (Figure S2D). HIF-1 α binding to the NDUFA4L2 proximal promoter containing conserved HRE site (A) was strongly induced by hypoxia and DMOG treatment (Figure 2E), but not to the non-conserved HRE site (B) or the negative control

region (C). The sequence amplified by qPCR had the expected size (Figure 2F). Taken together, these results suggest that NDUFA4L2 is a direct HIF-1 target gene.

NDUFA4L2 is involved in the hypoxia-induced decrease in oxygen consumption, and prevents increases in membrane potential and ROS production during hypoxia

To test whether NDUFA4L2 is involved in the regulation of mitochondrial activity in hypoxia, we first determined the oxygen consumption in HeLa cells in which NDUFA4L2 was silenced by specific siRNA. In these experiments, NDUFA4L2 expression was typically reduced by 80% in hypoxic conditions (Figure S3A) while NDUFA4 mRNA levels were not affected by the siNDUFA4L2 (Figure S3B), highlighting the specificity of the interference of NDUFA4L2. Indeed, NDUFA4L2 interference reduced its protein expression in both normoxic and hypoxic conditions (Figure 3A) whereas the expression levels of proteins from other ETC complexes were unaffected by NDUFA4L2 interference (Figures S3C). Oxygen consumption decreased approximately 42% in hypoxic conditions when compared to normoxia in control HeLa cells (Figure 3B). However, oxygen consumption only decreased by 27% in hypoxic conditions when NDUFA4L2 was silenced in HeLa cells and when compared to control cells in normoxic conditions (Figure 3B). In normoxia, NDUFA4L2 silencing increased oxygen consumption by only 10%, probably due to the low normoxic levels of NDUFA4L2. We also tested whether transient over-expression of NDUFA4L2 might decrease oxygen consumption by using a pCMV-NDUFA4L2 vector to achieve similar expression levels to those obtained in hypoxia (Figures

3C and S3D). Transient over-expression of NDUFA4L2 decreased oxygen consumption in HeLa cells by approximately 20% (Figure 3D). Hence, we conclude that during hypoxia, NDUFA4L2 induction decreases oxygen consumption.

Since attenuation of mitochondrial activity in hypoxia may be a compensatory mechanism to keep mitochondrial ROS under control, we wondered whether hypoxia-driven NDUFA4L2 up-regulation could also participate in this antioxidant response. Previous studies used the fluorescent dye H₂DCFDA and flow cytometry to demonstrate an increase of mitochondrial ROS production when cells are exposed to low O₂ tensions (Brunelle et al., 2005; Guzy et al., 2005; Mansfield et al., 2005). Accordingly, we observed increased H₂DCFDA fluorescence in HeLa cells exposed to hypoxia (1% O₂) that was exacerbated when NDUFA4L2 was silenced (Figure 3E). Similar data were obtained using the mitochondrial superoxide indicator MitoSOX (Figure 3F), which points to the mitochondrial origin of this increased superoxide production, probably from respiratory complexes. Increased ROS production in the absence of NDUFA4L2 during hypoxia correlated with an increased mitochondrial membrane potential in these conditions (Figure 3G). Conversely, NDUFA4L2 overexpression significantly decreased membrane potential compared to cells expressing the empty vector (Figure 3H).

The hypoxia-induced decrease in oxygen consumption via NDUFA4L2 occurs through Complex I inhibition

Given that NDUFA4L2 appears to be a mitochondrial protein involved in the down-regulation of hypoxia-induced oxygen consumption and that it likely

belongs to the NDUFA4 subunit family of Complex I, we wondered whether NDUFA4L2 might be involved in actively regulating Complex I activity. We found that, when compared to normoxic conditions, Complex I activity decreased ~20% in HeLa cells exposed to hypoxia (1% O₂ for 24 h), although it not when NDUFA4L2 expression was silenced (Figure 4A). Moreover, transient over-expression of NDUFA4L2 decreased Complex I activity in normoxic conditions (Figure 4B) demonstrating that NDUFA4L2 regulates Complex I under low oxygen conditions.

To study the specificity of the effects of NDUFA4L2 on Complex I, we also measured Complex IV activity. Hypoxia (1% O₂ for 24 h) induced a 38% decrease in Complex IV activity in HeLa cells (Figure 4C) but the silencing of NDUFA4L2 expression in hypoxia, or its over-expression in normoxia, did not affect Complex IV activity (Figures 4C and 4D). Similar results were obtained when Complex IV activity was determined spectrophotometrically (data not shown). Hence, NDUFA4L2 appears to affect ETC activity by specifically inhibiting Complex I. Since our results indicate that NDUFA4L2 is a HIF-1 α dependent gene involved in the down-regulation of Complex I activity in hypoxia, we further studied the role of HIF1 in regulating Complex I. As expected, there was no decrease in Complex I activity following hypoxia in tamoxifen treated Hif1 $\alpha^{+/f}/$ Cre MEFs in which HIF-1 α was ablated (Figure 4E). By contrast, a similar decrease in Complex I activity to that seen in HeLa cells was evident in tamoxifen treated Hif1 $\alpha^{+/+}/$ Cre MEFs (~20%; Figure 4F). These results suggest that the HIF-1 α induced increase in NDUFA4L2 expression decreased oxygen consumption through the specific inhibition of mitochondrial Complex I activity.

Complex I activity can be modulated by its assembly (Vogel et al., 2005). We hypothesized that hypoxia-induced NDUFA4L2 could affect Complex I assembly. To test this possibility, we performed Blue native PAGE (BN-PAGE) in order to analyze the status of mitochondrial complexes. Neither hypoxia nor NDUFA4L2 silencing modified Complex I content, thus ruling out the involvement of NDUFA4L2 in the Complex I assembly process (Figure 4G).

Silencing of NDUFA4L2 impairs cell proliferation in hypoxia by increasing mitochondrial ROS generation

While the absence of NDUFA4L2 does not significantly affect cell proliferation in normoxic conditions (Figure 5A), viable hypoxic NDUFA4L2-silenced HeLa cells proliferated at a slower rate than hypoxic control cells (Figure 5B). This slower proliferation was evident by both cell counting and by direct observation under the microscope (Figure 5C); it was also observed in other cell types such as HUVEC, UCD-Mel-N and SKOV3 cells (Figure S4A). NDUFA4L2-silenced cells did not show either increased caspase-3 cleavage (Figure 5D) or changes in propidium iodide incorporation (Figure 5E), excluding the possibility that NDUFA4L2 silencing impaired cell proliferation by activating apoptosis. Additional studies showed that the capacity of hypoxic HeLa cells to form colonies in soft agar was affected when NDUFA4L2 was silenced, with a decrease in both the size and the number of colonies (Figure 5F). In order to investigate whether ROS overproduction in NDUFA4L2-silenced HeLa cells during hypoxia was responsible for the impairment in cell proliferation, we tested the effects of two different antioxidants, N-acetylcysteine (NAC) and MitoQ (an antioxidant targeted to mitochondria), on cell proliferation. Cell

proliferation was restored when NDUFA4L2-silenced HeLa cells were treated with MitoQ in hypoxia (Figure 5G). This effect was also observed with NAC (Figure S4B), suggesting that exacerbated ROS production may be involved in the impairment of cell viability under hypoxia. Indeed, an increase in ROS production was detected in NDUFA4L2-silenced cells exposed to hypoxia using the mitochondrial superoxide indicator MitoSOX (Figure 5H). This increase was completely prevented by incubation with MitoQ (Figure 5H).

Cell cycle analysis showed that hypoxic NDUFA4L2-silenced HeLa cells had increased early S phase and decreased late S phase compared to scramble control cells (Figure S4C). Since NDUFA4L2-silenced HeLa cells present ROS overproduction in hypoxia, and ROS can increase the phosphorylation of histone H2AX, a marker of cell stress (Driessens et al., 2009), we then analyzed the phosphorylation of H2AX histone. We observed increased phospho-H2AX levels in hypoxia when NDUFA4L2 was interfered (Figure S4D), suggesting that the lack of NDUFA4L2 in hypoxia produces cell stress.

It has been described that both the down-regulation of ISCU 1/2 via miR-210 and the up-regulation of PDK1 are implicated in ROS control and cell viability in hypoxia (Chan et al., 2009; Chen et al., 2010; Favaro et al., 2010; Kim et al., 2006; Papandreou et al., 2006). To investigate the relative contribution of these effects to HeLa hypoxic adaptation we performed cell proliferation assays. We only observed a decrease in ISCU 1/2 protein at times over 24 h at 0.5% (Figure S5A) but not in the milder hypoxic conditions (1% O₂). Furthermore, the overexpression of ISCU 1/2 did not affect HeLa cell

proliferation in hypoxia (0.5% O₂) at 72 h (Figure S5B). In addition, HeLa cells in which PDK1 was silenced by specific siRNA (Figure S5C) showed a decrease in proliferation under hypoxia (0.5% O₂) at 72 h (Figure S5D) similar to that observed in NDUFA4L2-silenced cells, suggesting that both NDUFA4L2 and PDK1 play an important role in ROS control and cell proliferation in our system conditions.

MEFs obtained from NDUFA4L2 knockout mice exhibit higher oxygen consumption and Complex I activity in hypoxia than wild-type MEFs

In order to gain further insight into the role of NDUFA4L2 on hypoxia-induced mitochondrial reprogramming, we generated NDUFA4L2 knock-out mice. We initially planned to isolate primary cell cultures from NDUFA4L2 deficient adult mice. However, we found that homozygous NDUFA4L2 gene inactivation results in perinatal lethality, which demonstrates an essential biological role of NDUFA4L2 in development that will be further explored in future studies. Therefore we isolated NDUFA4L2 deficient MEFs and the corresponding wild type controls from E12.5 -14.5 embryos generated from NDUFA4L2^{+/-} breeding pairs. In order to validate these MEFs cultures we analyzed the expression of NDUFA4L2. Western blot analysis confirmed that NDUFA4L2 increased in hypoxia in MEFs from wild-type mice only (Figure 6A). We determined oxygen consumption in MEFs obtained from NDUFA4L2 knockout and wild-type mice (Figure 6B). Confirming results obtained in HeLa cells, MEFs from NDUFA4L2 KO mice showed increased respiration rate in hypoxia compared to wild-type mice (Figure 6B). The activity of Complex I in hypoxia was higher in MEFs from KO mice than in those from wild-type mice, confirming the results obtained in

HeLa cells (Figure 6C). In contrast, the activity of Complex IV in hypoxia was similarly decreased in both types of MEFs (Figure 6D). The expression level of respiratory complexes was studied by BN-PAGE using DDM (n-dodecyl beta-D-maltoside) obtaining the same result as in HeLa cells (data not shown). In addition, MEFs from NDUFA4L2 KO mice exhibited a lower proliferation rate than those from wild-type mice when cultured under hypoxia (Figure 6E) and this lower proliferation correlated with increased ROS production under hypoxic conditions (Figure 6F).

NDUFA4 paralogue is repressed under hypoxia at the protein level

It is established that a COX4-2 to COX4-1 subunit substitution takes place at Complex IV during hypoxia (Fukuda et al., 2007). The paralogue proteins NDUFA4L2 and NDUFA4 derive from the same ancestral gene, share more than 65% in their amino acid sequence and have been suggested to be part of mitochondrial Complex I (Walker et al., 1992). Since NDUFA4 mRNA level does not change in hypoxia up to 48 h (Figure 7A), we investigated the fate of the protein under hypoxia. We found that NDUFA4 protein decreases in hypoxic cells while NDUFA4L2 protein expression increases in hypoxic conditions (Figure 7B). We also explored whether NDUFA4L2 levels would be responsible for the down-regulation of NDUFA4. NDUFA4 protein levels decreased in hypoxia even when NDUFA4L2 was silenced (Figure 7C), and its expression in normoxia was unaffected by NDUFA4L2 overexpression (Figure 7D). NDUFA4 protein decreases to the same extent in NDUFA4L2 knockout MEFs demonstrating that both events occur independently (Figure 7E). Collectively all

these data indicate that NDUFA4L2 knockout MEFs markedly repress NDUFA4 protein levels in hypoxia while Complex I activity is not affected ruling out the possibility that Complex I activity is repressed in hypoxia via NDUFA4. These data stress the specific role of hypoxia-dependent NDUFA4L2 up-regulation in Complex I activity inhibition.

Discussion

The influence of fluctuations in oxygen concentration on mitochondrial activity has raised a great interest due to its broad impact on pathophysiology. Mitochondrial respiration is only compromised when the oxygen concentration drops below 0.1% O₂ because of the high affinity of mitochondrial cytochrome c oxidase (Complex IV) for oxygen (Aguirre et al., 2010; Gnaiger et al., 1998; Smolenski et al., 1991; Stumpe and Schrader, 1997). However, during moderate hypoxia (1-2% O₂), cells express a large number of genes, dependent on HIFs, that reprogram the metabolism to attenuate mitochondrial O₂ consumption, which also protects cells against excessive mitochondrial ROS formation (Aragones et al., 2009; Kim et al., 2006; Papandreou et al., 2006).

At the molecular level, we show here that moderate hypoxia decreases oxygen consumption and Complex I activity via the HIF-1-dependent up-regulation of NDUFA4L2. Our data indicate that NDUFA4L2 is a HIF-1-dependent gene, emphasizing the role of HIF-1 in mitochondrial reprogramming and revealing NDUFA4L2 as an important element in metabolic adaptation to hypoxia. We have observed this induction in different cell types, as well as in tissue from animals subjected to hypoxia, suggesting a role in physiological adaptation to hypoxia. In this regard, NDUFA4L2 knockout homozygous mice,

which could be a presumed mouse model of Complex I gain of function based on our own data, show perinatal lethality, stressing the high relevance of this protein *in vivo*. Similarly, mouse models of Complex I deficiency (Kruse et al., 2008) also die shortly after birth which indicates that Complex I activity needs to be tightly controlled to assure an adequate development early after birth.

The PHD oxygen-sensing pathway is also known to up-regulate the pyruvate dehydrogenase kinase isoforms PDK1, PDK3 and PDK4 (Aragones et al., 2008; Kim et al., 2006; Lu et al., 2008; Papandreou et al., 2006). PDK overactivation reduces pyruvate dehydrogenase (PDH) activity, slowing down the conversion of pyruvate into acetyl-CoA and ultimately repressing the TCA cycle and the supply of NADH to the mitochondrial ETC. Therefore, PDKs could potentially cooperate with NDUFA4L2 to reduce mitochondrial Complex I activity under moderate hypoxic conditions, but it is also conceivable that NDUFA4L2 has other biological functions that cannot be accomplished by PDKs. For example, when metabolites that fuel the TCA cycle originate from pathways different from glycolysis (e.g. glutaminolysis or fatty acid oxidation), it would be necessary to reduce ETC activity in order to decrease mitochondrial function (Wheaton and Chandel, 2011). Hypoxia-induced NDUFA4L2 expression could fulfill this role reducing oxygen consumption due to its strategic position downstream of the TCA cycle, possibly at Complex I (Figure 7F). Likewise, hypoxia induces the up-regulation of microRNA-210, which represses the iron-sulfur cluster assembly proteins (ISCU1/2) (Chan et al., 2009; Chen et al., 2010; Favaro et al., 2010). These proteins facilitate the assembly of iron-sulfur clusters, including those in Complex I, Complex III and aconitase, which are critical for electron transport and mitochondrial redox

reactions. As a result, microRNA-210 represses mitochondrial respiration. In our model, and in line with previous studies, ISCU1/2 protein does not decrease prior 48 h and only under 0.5% O₂, while NDUFA4L2 becomes functional as early as 24 h at 1% O₂. Moreover, ISCU1/2 recovery in hypoxic HeLa cells did not disturb proliferation. In this sense, it has been described that an anti-miR-210 affects HeLa cell proliferation at times longer than 48 h and at very low oxygen tensions (0.01% O₂) (Favaro et al., 2010).

Very intriguing however, Complex I inhibition, in HeLa cells, takes place at milder hypoxia (1% O₂) (Figures 4) and this oxygen tension does not seem to be enough to decrease ISCU1/2 (Figures 5S). Furthermore, ISCU1/2 downregulation is not observed before 48 hours but Complex I is inhibited as early as 24 hours. This opened a 24h-window where not known player was involved, until now. NDUFA4L2 early induction fits in this model. As demonstrated, NDUFA4L2 Complex I inhibition occurs without affecting Complex I quantity, but probably by a direct or indirect interaction which remains to be elucidated. However miRNA210 targeted ISCU1/2 presumably fulfill its function by decreasing Complex I content. This early NDUFA4L2-dependent qualitative modulation followed by a later miR210-dependent quantitative repression of Complex I represent a possible model by which HIF-1 guarantee a fine control of Complex I under hypoxic conditions. In summary, we propose that, although NDUFA4L2 upregulation and miR210-induced ISCU1/2 repression could act synergistically to decrease Complex I activity and oxygen consumption in chronic hypoxia, we should underscore that primary (1% O₂) Complex I inhibition can be only accomplished by early NDUFA4L2 induction.

Altered subunit content during hypoxia has also been reported for other ETC complexes. Thus, physiological hypoxia induces a COX4-1 to COX4-2 subunit switch, an effect mediated by HIF-1 which is thought to optimize the efficiency of respiration during conditions of reduced oxygen availability (Fukuda et al., 2007). Since we have found that NDUFA4 is down-regulated at the protein level in hypoxia, we could speculate that NDUFA4L2 induction is taking over NDUFA4 place at Complex I and reducing in some way its activity. However, NDUFA4L2 knockout MEFs markedly repress NDUFA4 protein levels in hypoxia while Complex I activity is not affected, ruling out the possibility that Complex I activity is repressed in hypoxia via NDUFA4. In this regard, the role and location of NDUFA4 within Complex I are not yet well understood.

The ETC produces superoxide when single electrons are transferred to O₂ during electron transport. There are different sites of ROS production in mammalian mitochondria (Murphy, 2009), but the greatest maximum capacity of ROS production are the ubiquinone reduction site of Complex I and the outer quinone-binding site of the Q cycle in Complex III (Liu et al., 2002; Raha and Robinson, 2000; St-Pierre et al., 2002; Votyakova and Reynolds, 2001). Although superoxide production in isolated mitochondria correlates with oxygen tension (Liu et al., 2002), it is generally accepted that ROS production in cells increases during short periods of hypoxia (Brunelle et al., 2005; Guzy et al., 2005; Mansfield et al., 2005). In agreement with this, we detected increased ROS in hypoxia using the fluorescent probes DCFDA and MitoSOX. The hypoxia-induced ROS increase was exacerbated in the absence of NDUFA4L2 indicating that the expression of this protein keeps ROS production under control and hence could protect the cell against oxidative stress. Whether the

effects of NDUFA4L2 on ROS production are direct or occur through the modulation of other mitochondrial proteins requires further research. However, the fact that mitochondrial membrane potential increases simultaneously with increased ROS in the absence of NDUFA4L2 suggests that both events might be closely associated, as has been demonstrated elsewhere (Korshunov et al., 1997; Votyakova and Reynolds, 2001).

Hypoxia-exposed cell cultures accumulate intracellular ROS but most probably at lower sub-lethal concentrations. As shown in Figure 5, and in line with previous studies, hypoxia slows down proliferation (Gardner et al., 2001; Goda et al., 2003). However, NDUFA4L2-silenced cells and MEFs from NDUFA4L2 KO mice showed a more profound inhibition of cell proliferation in parallel to a higher ROS accumulation and DNA stress/damage (H2AX phosphorylation) than control cells or MEFs from wild-type mice. NDUFA4L2-silenced cells did not show signs of cellular apoptosis, probably because of the high resistance-nature of this tumor cells. Therefore, it is reasonable to think that PHD-HIF system counteracts ROS overproduction that impairs cell growth.

Several *in vivo and in vitro* studies have revealed that the reduction of mitochondrial oxygen consumption through PHD and HIF activities prepares cells to tolerate more extreme lethal hypoxic/ischemic conditions, saving oxygen and reducing mitochondrial ROS formation. We hypothesize that NDUFA4L2 induction during hypoxia helps keeping intracellular ROS production in check, consistent with the fact that NDUFA4L2 limits Complex I activity and prevents increases in membrane potential. It is therefore reasonable to speculate that NDUFA4L2 could participate in ischemic preconditioning. Indeed, several *in*

in vivo studies have shown that partial inhibition of Complex I with sub-lethal doses of amobarbital (a reversible inhibitor at the rotenone site of Complex I) prevents reperfusion-induced cardiac damage (Aldakkak et al., 2008; Chen et al., 2006a; Chen et al., 2006b).

Our studies indicate that mitochondrial Complex I activity is controlled by NDUFA4L2 during hypoxia. In conjunction with previous data on PHD and HIF-regulated mitochondrial activity, we add further elements to the strategic armory used by HIFs to ensure that mitochondrial oxygen consumption is repressed in mild hypoxic conditions, highlighting the biological relevance of the regulation of this cellular response.

Experimental Procedures

Cell lines and cultures. HeLa, RCC4, RCC4/VHL, PC-12, HL-1, neonatal rat cardiomyocytes, Hif1 $\alpha^{+/+}$ /Cre or Hif1 $\alpha^{+f/+f}$ /Cre mouse embryo fibroblasts (MEFs) and Human umbilical vein endothelial cells (HUVEC) were used. See *SI Methods* for details.

Microarray analysis

Total RNA was extracted using Ultraspec reagent (Biotechx, Houston, TX). One-Color Microarray-Based Gene Expression Analysis Protocol (Agilent Technologies, Palo Alto, CA, USA) was used to amplify and label RNA. Briefly, 200-700 ng of total RNA was reverse transcribed using T7 promoter Primer and MMLV-RT. Then cDNA was converted to aRNA using T7 RNA polymerase,

which simultaneously amplifies target material and incorporates cyanine 3-labeled CTP. Samples were hybridized to Whole Human Genome Microarray 4 x 44K (G4112F, Agilent Technologies). 1.65 g of Cy3 labelled aRNA were hybridized for 17 hours at 65°C in a hybridization oven (G2545A, Agilent) set to 10 rpm in a final concentration of 1X GEx Hybridization Buffer HI-RPM, according to manufacturer's instructions (One-Color Microarray-Based Gene Expression Analysis, Agilent Technologies). Arrays were washed according to manufacturer's instructions (One-Color Microarray-Based Gene Expression Analysis, Agilent Technologies) and dried out using a centrifuge. Finally arrays were scanned at 5 m resolution on an Agilent DNA Microarray Scanner (G2565BA, Agilent Technologies) using the default settings for 4x44k format one-color arrays. Images provided by the scanner were analyzed using Feature Extraction software version 9.5.3.1 (Agilent Technologies).

***In vivo* hypoxia experiments.** Eight-week-old male C57BL/6 mice were exposed to hypoxic (7.5% O₂) or normoxic (21% O₂) conditions for 18 h.. After treatment mice were sacrificed under the same conditions to avoid tissue reoxygenation following hypoxia. The brain and heart were then excised, frozen in liquid nitrogen and stored at -80 °C. Organs were homogenized in liquid nitrogen and resuspended in RIPA buffer (1% NP40, 0.5% sodium deoxycholate and 0.1% SDS in PBS buffer) for protein extraction or Ultraspec reagent (Biotechx, Houston, TX) for mRNA isolation.

Oxygen consumption. Oxygen consumption was determined by high-resolution respirometry (Oxygraph-2k, Oroboros Instruments, Innsbruck, Austria). Cells were trypsinized after the indicated treatments and then

resuspended at 2×10^6 cells/ml in HBSS containing 25 mM Hepes. The instrumental background flux was calculated as a linear function of the oxygen concentration and the experimental data were corrected using DatLab software (Oroboros Instruments). The oxygen concentration in air saturated culture medium at 37°C was 175.7 μ M (Rodriguez-Juarez et al., 2007). Measurements were taken at 37°C in parallel Oxygraph-2k chambers for cells incubated in normoxic and hypoxic (1% O₂) conditions with the indicated treatments.

Mitochondria isolation. The isolation of an enriched mitochondrial fraction from 2.5×10^7 HeLa cells was performed using the Mitochondria Isolation Kit MITOISO2 (Sigma) according to the manufacturer's instructions.

Complex I and IV activity. The activities of Complex I and Complex IV were measured using the Complex I Enzyme Activity Microplate Assay Kit or the Complex IV Human Duplexing Microplate Assay Kit, both from MitoSciences, according to the manufacturer's instructions.

Mitochondrial membrane potential. Mitochondrial membrane potential was determined by incubating the cells with the fluorescent dye tetramethylrhodamine ethyl ester (TMRE; Sigma). Cells were incubated with 2.5 nM TMRE for 30 min at 37°C and subsequently analyzed by FACScan flow cytometer (Becton Dickinson, Lincoln Park, NJ).

Cell proliferation and apoptosis. For the cell proliferation assay, 2×10^5 HeLa, HUVEC, UCD-mel-N and SKOV3 cells were planted in a 10 cm dish 1 day before exposure to hypoxic conditions (0.5% O₂). 0.1 mM N-acetylcysteine (NAC) or 0.5 μ M Mito-Q (0.5 μ M DTPP was used as control of Mito-Q) was

added to HeLa cells to determinate the effect of the antioxidants on NDUFA4L2 interfered cells proliferation in hypoxia. At the times indicated, the cells were trypsinized and the viable cells were counted using trypan blue. Apoptosis was determined by flow cytometry analysis of the cell cycle after DNA staining with propidium iodide (PI), and by analysis of cleaved caspase-3 with a specific antibody (Cell Signaling). Positive controls for apoptosis were performed by incubating HeLa cells with taxol (Calbiochem) at 1µg/ml for 18 h.

Soft agar assay. HeLa cells were seeded into 0.35% agar Noble (Difco) in DMEM containing 10% heat-inactivated FBS on top of a bed of 0.5% agar in 60-mm dishes at 5×10^3 cells per dish. Immobilized cells were grown for 15 days in a humidified chamber at 37 °C and exposed to normoxic or hypoxic conditions (0.5% O₂). Colonies were then photographed using a DS-Fi1 camera (Nikon) and were then counted and measured using imageJ software.

Analysis of electron transport chain complexes by Blue-Native electrophoresis gel (BNGE) Mitochondrial membrane proteins (100–150 mg) were applied and run on a 3%–13% first-dimension gradient BNGE gel as described elsewhere).(Schagger, 1995). After electrophoresis, the complexes were electroblotted onto PVDF filters and sequentially probed with specific antibodies against complex I, and NDUFA9 (Molecular Probes); complex III, anti-core2 (Molecular Probes); complex IV, anti-COI (Molecular Probes); complex II.

NDUFA4L2 gene inactivation in mice. NDUFA4L2 chimeric males were obtained from Velocigene Regeneron Pharmaceuticals, Inc. (Reference number: 13661) through the KOMP repository. These chimeric mice were

crossed with wild type C57BL/6 females to generate NDUFA4L2 heterocygous mice. NDUFA4L2 heterocygous mice were used to generate NDUFA4L2 deficient embryos and the subsequent murine embryonic fibroblast isolation. The mice were bred and housed in a specific pathogen free (SPF) animal area of the animal facility at the Autonomous University of Madrid (UAM).

Statistical analysis. The data are presented as the means \pm SEM of at least three independent experiments. Statistical significance (*, $p < 0.05$) or (**, $p < 0.01$) was assessed by the Wilcoxon test.

Acknowledgements. This work was supported by Ministerio de Ciencia y Tecnología (SAF 2007-06592), (SAF 2010-14851) Comunidad Autónoma de Madrid (SAL-0311-2006), Metoxia Project-Health (F2 2009-222741) and Recava Network (RD 06/0014/0031) to M.L., CP07/00143, PS09/00101 and CSD2007-00020 to A.M.R., PI060701, PS09/00116 and CP08/00204 to S.C. and BFU2008-03407/BMC to J.A. We are grateful to Mike Murphy (Mitochondrial Biology Unit, MRC, Cambridge, UK) for the gift of MitoQ. We also thank Stephen Y. Chan and Joseph Loscalzo (Harvard Medical School, Boston, MA, USA) for providing us ISCU expression vectors.

References

- Aguirre, E., Rodriguez-Juarez, F., Bellelli, A., Gnaiger, E., and Cadenas, S. (2010). Kinetic model of the inhibition of respiration by endogenous nitric oxide in intact cells. *Biochimica et biophysica acta* 1797, 557-565.
- Aldakkak, M., Stowe, D.F., Chen, Q., Lesnefsky, E.J., and Camara, A.K. (2008). Inhibited mitochondrial respiration by amobarbital during cardiac ischaemia improves redox state and reduces matrix Ca^{2+} overload and ROS release. *Cardiovascular research* 77, 406-415.
- Andreas, K., Haupl, T., Lubke, C., Ringe, J., Morawietz, L., Wachtel, A., Sittlinger, M., and Kaps, C. (2009). Antirheumatic drug response signatures in human chondrocytes:

potential molecular targets to stimulate cartilage regeneration. *Arthritis research & therapy* 11, R15.

Aragones, J., Fraisl, P., Baes, M., and Carmeliet, P. (2009). Oxygen sensors at the crossroad of metabolism. *Cell metabolism* 9, 11-22.

Aragones, J., Schneider, M., Van Geyte, K., Fraisl, P., Dresselaers, T., Mazzone, M., Dirkx, R., Zacchigna, S., Lemieux, H., Jeoung, N.H., et al. (2008). Deficiency or inhibition of oxygen sensor Phd1 induces hypoxia tolerance by reprogramming basal metabolism. *Nat Genet* 40, 170-180.

Brunelle, J.K., Bell, E.L., Quesada, N.M., Vercauteren, K., Tiranti, V., Zeviani, M., Scarpulla, R.C., and Chandel, N.S. (2005). Oxygen sensing requires mitochondrial ROS but not oxidative phosphorylation. *Cell metabolism* 1, 409-414.

Carroll, J., Fearnley, I.M., Skehel, J.M., Shannon, R.J., Hirst, J., and Walker, J.E. (2006). Bovine complex I is a complex of 45 different subunits. *The Journal of biological chemistry* 281, 32724-32727.

Chan, S.Y., Zhang, Y.Y., Hemann, C., Mahoney, C.E., Zweier, J.L., and Loscalzo, J. (2009). MicroRNA-210 controls mitochondrial metabolism during hypoxia by repressing the iron-sulfur cluster assembly proteins ISCU1/2. *Cell metabolism* 10, 273-284.

Chen, Q., Hoppel, C.L., and Lesnefsky, E.J. (2006a). Blockade of electron transport before cardiac ischemia with the reversible inhibitor amobarbital protects rat heart mitochondria. *The Journal of pharmacology and experimental therapeutics* 316, 200-207.

Chen, Q., Moghaddas, S., Hoppel, C.L., and Lesnefsky, E.J. (2006b). Reversible blockade of electron transport during ischemia protects mitochondria and decreases myocardial injury following reperfusion. *The Journal of pharmacology and experimental therapeutics* 319, 1405-1412.

Chen, Z., Li, Y., Zhang, H., Huang, P., and Luthra, R. (2010). Hypoxia-regulated microRNA-210 modulates mitochondrial function and decreases ISCU and COX10 expression. *Oncogene* 29, 4362-4368.

Driessens, N., Versteyhe, S., Ghaddhab, C., Burniat, A., De Deken, X., Van Sande, J., Dumont, J.E., Miot, F., and Corvilain, B. (2009). Hydrogen peroxide induces DNA single- and double-strand breaks in thyroid cells and is therefore a potential mutagen for this organ. *Endocr Relat Cancer* 16, 845-856.

Favaro, E., Ramachandran, A., McCormick, R., Gee, H., Blancher, C., Crosby, M., Devlin, C., Blick, C., Buffa, F., Li, J.L., et al. (2010). MicroRNA-210 regulates mitochondrial free radical response to hypoxia and krebs cycle in cancer cells by targeting iron sulfur cluster protein ISCU. *PloS one* 5, e10345.

Favier, J., Briere, J.J., Burnichon, N., Riviere, J., Vescovo, L., Benit, P., Giscos-Douriez, I., De Reynies, A., Bertherat, J., Badoual, C., et al. (2009). The warburg effect is genetically determined in inherited pheochromocytomas. *PloS one* 4, e7094.

Fredlund, E., Ovenberger, M., Borg, K., and Pahlman, S. (2008). Transcriptional adaptation of neuroblastoma cells to hypoxia. *Biochemical and biophysical research communications* 366, 1054-1060.

Frost, M.T., Wang, Q., Moncada, S., and Singer, M. (2005). Hypoxia accelerates nitric oxide-dependent inhibition of mitochondrial complex I in activated macrophages. *American journal of physiology* 288, R394-400.

Fukuda, R., Zhang, H., Kim, J.W., Shimoda, L., Dang, C.V., and Semenza, G.L. (2007). HIF-1 regulates cytochrome oxidase subunits to optimize efficiency of respiration in hypoxic cells. *Cell* 129, 111-122.

Gardner, L.B., Li, Q., Park, M.S., Flanagan, W.M., Semenza, G.L., and Dang, C.V. (2001). Hypoxia inhibits G1/S transition through regulation of p27 expression. *The Journal of biological chemistry* 276, 7919-7926.

Gnaiger, E., Lassnig, B., Kuznetsov, A.V., and Margreiter, R. (1998). Mitochondrial respiration in the low oxygen environment of the cell. Effect of ADP on oxygen kinetics. *Biochimica et biophysica acta* 1365, 249-254.

Goda, N., Ryan, H.E., Khadivi, B., McNulty, W., Rickert, R.C., and Johnson, R.S. (2003). Hypoxia-inducible factor 1 α is essential for cell cycle arrest during hypoxia. *Molecular and cellular biology* 23, 359-369.

Guzy, R.D., Hoyos, B., Robin, E., Chen, H., Liu, L., Mansfield, K.D., Simon, M.C., Hammerling, U., and Schumacker, P.T. (2005). Mitochondrial complex III is required for hypoxia-induced ROS production and cellular oxygen sensing. *Cell metabolism* 1, 401-408.

Iyer, N.V., Kotch, L.E., Agani, F., Leung, S.W., Laughner, E., Wenger, R.H., Gassmann, M., Gearhart, J.D., Lawler, A.M., Yu, A.Y., et al. (1998). Cellular and developmental control of O₂ homeostasis by hypoxia-inducible factor 1 α . *Genes & development* 12, 149-162.

Kaelin, W.G., Jr., and Ratcliffe, P.J. (2008). Oxygen sensing by metazoans: the central role of the HIF hydroxylase pathway. *Mol Cell* 30, 393-402.

Kim, J.W., Tchernyshyov, I., Semenza, G.L., and Dang, C.V. (2006). HIF-1-mediated expression of pyruvate dehydrogenase kinase: a metabolic switch required for cellular adaptation to hypoxia. *Cell metabolism* 3, 177-185.

Korshunov, S.S., Skulachev, V.P., and Starkov, A.A. (1997). High protonic potential actuates a mechanism of production of reactive oxygen species in mitochondria. *FEBS Lett* 416, 15-18.

Kruse, S.E., Watt, W.C., Marcinek, D.J., Kapur, R.P., Schenkman, K.A., and Palmiter, R.D. (2008). Mice with mitochondrial complex I deficiency develop a fatal encephalomyopathy. *Cell metabolism* 7, 312-320.

Liu, Y., Fiskum, G., and Schubert, D. (2002). Generation of reactive oxygen species by the mitochondrial electron transport chain. *J Neurochem* 80, 780-787.

Lu, C.W., Lin, S.C., Chen, K.F., Lai, Y.Y., and Tsai, S.J. (2008). Induction of pyruvate dehydrogenase kinase-3 by hypoxia-inducible factor-1 promotes metabolic switch and drug resistance. *The Journal of biological chemistry* 283, 28106-28114.

Mansfield, K.D., Guzy, R.D., Pan, Y., Young, R.M., Cash, T.P., Schumacker, P.T., and Simon, M.C. (2005). Mitochondrial dysfunction resulting from loss of cytochrome c impairs cellular oxygen sensing and hypoxic HIF- α activation. *Cell metabolism* 1, 393-399.

Murphy, M.P. (2009). How mitochondria produce reactive oxygen species. *The Biochemical journal* 417, 1-13.

Papandreou, I., Cairns, R.A., Fontana, L., Lim, A.L., and Denko, N.C. (2006). HIF-1 mediates adaptation to hypoxia by actively downregulating mitochondrial oxygen consumption. *Cell metabolism* 3, 187-197.

Piruat, J.I., and Lopez-Barneo, J. (2005). Oxygen tension regulates mitochondrial DNA-encoded complex I gene expression. *The Journal of biological chemistry* 280, 42676-42684.

Raha, S., and Robinson, B.H. (2000). Mitochondria, oxygen free radicals, disease and ageing. *Trends Biochem Sci* 25, 502-508.

Rodriguez-Juarez, F., Aguirre, E., and Cadenas, S. (2007). Relative sensitivity of soluble guanylate cyclase and mitochondrial respiration to endogenous nitric oxide at physiological oxygen concentration. *The Biochemical journal* 405, 223-231.

Schagger, H. (1995). Native electrophoresis for isolation of mitochondrial oxidative phosphorylation protein complexes. *Methods Enzymol* 260, 190-202.

Schofield, C.J., and Ratcliffe, P.J. (2004). Oxygen sensing by HIF hydroxylases. *Nature reviews* 5, 343-354.

Semenza, G.L. (2004). Hydroxylation of HIF-1: oxygen sensing at the molecular level. *Physiology* 19, 176-182.

Semenza, G.L. (2009). Regulation of oxygen homeostasis by hypoxia-inducible factor 1. *Physiology* 24, 97-106.

Smolenski, R.T., Schrader, J., de Groot, H., and Deussen, A. (1991). Oxygen partial pressure and free intracellular adenosine of isolated cardiomyocytes. *Am J Physiol* 260, C708-714.

St-Pierre, J., Buckingham, J.A., Roebuck, S.J., and Brand, M.D. (2002). Topology of superoxide production from different sites in the mitochondrial electron transport chain. *The Journal of biological chemistry* 277, 44784-44790.

Stumpe, T., and Schrader, J. (1997). Phosphorylation potential, adenosine formation, and critical PO₂ in stimulated rat cardiomyocytes. *Am J Physiol* 273, H756-766.

Vogel, R.O., Janssen, R.J., Ugalde, C., Grovenstein, M., Huijbens, R.J., Visch, H.J., van den Heuvel, L.P., Willems, P.H., Zeviani, M., Smeitink, J.A., et al. (2005). Human mitochondrial complex I assembly is mediated by NDUFAF1. *Febs J* 272, 5317-5326.

Votyakova, T.V., and Reynolds, I.J. (2001). DeltaPsi(m)-Dependent and -independent production of reactive oxygen species by rat brain mitochondria. *J Neurochem* 79, 266-277.

Walker, J.E., Arizmendi, J.M., Dupuis, A., Fearnley, I.M., Finel, M., Medd, S.M., Pilkington, S.J., Runswick, M.J., and Skehel, J.M. (1992). Sequences of 20 subunits of NADH:ubiquinone oxidoreductase from bovine heart mitochondria. Application of a novel strategy for sequencing proteins using the polymerase chain reaction. *J Mol Biol* 226, 1051-1072.

Wheaton, W.W., and Chandel, N.S. (2011). Hypoxia. 2. Hypoxia regulates cellular metabolism. *Am J Physiol Cell Physiol* 300, C385-393.

Figure Legends

Figure 1. NDUFA4L2 localizes to mitochondria and it is induced in tumor cells, primary cultures and *in vivo* by hypoxia. (A-C) Quantitative RT-PCR analysis of *NDUFA4L2* mRNA expression relative to the values in normoxia. (A-B) HeLa, PC-12, cardiomyocytes and HUVEC were cultured under conditions of normoxia or hypoxia (1% O₂) for 6 (HeLa) or 18 h (PC-12, cardiomyocytes, HUVEC). DMOG was added at 1 mM (cardiomyocytes) or 0.1 mM (HUVEC) and deferroxamine (DFO) was added at 0.2 mM in HUVEC (n=3). (C) Brain tissue from mice exposed to normoxic (n=8) or hypoxic (7.5% O₂; n=7) conditions for 18 h. (D) Immunoblot assay of NDUFA4L2 protein in HeLa, PC-12, HUVEC, rat cardiomyocytes cultured under normoxic or hypoxic conditions (1% O₂ for cell cultures), as well as in brain tissue of mice subjected to hypoxia (7.5% O₂) for 18 h. Tubulin is shown as a loading control. The images are representative of at least 3 experiments. (E) Immunofluorescence showing the increase in NDUFA4L2 protein levels in rat cardiomyocytes exposed to normoxia or hypoxia (1% O₂) for 18 h, with respect to those maintained in normoxic conditions. The images shown are representative of 3 experiments. (F) Immunoblot assay of NDUFA4L2 in total cell (T), cytoplasmic (C) and mitochondrial (M) protein extracts from HeLa cells cultured under normoxic or

hypoxic conditions (1% O₂) for 18 h. Cytochrome c was assayed as a mitochondrial marker. The images shown are representative of 3 experiments. (G) Immunofluorescence of HL-1 cells exposed to normoxia or hypoxia (1% O₂) for 18 h. Images show staining for NDUFA4L2 (left panel, green), Cytochrome c (middle panel, red) and an overlay of the two signals (right panel). The images shown are representative of 3 experiments. See also Figure S1. (n>3; mean ± SEM; *, p<0.05; **, p<0.01).

Figure 2. NDUFA4L2 induction is mediated by HIF-1α. (A) HeLa cells transfected with siRNA against HIFβ or a scramble control were cultured under normoxic or hypoxic (1% O₂) conditions for 24 h. NDUFA4L2 mRNA levels were quantified by real-time RT-PCR. (B) VHL-deficient RCC4 cells or RCC4/VHL cells were transfected with siRNA against HIF-1α, HIF-2α or a scramble control and exposed under normoxic or hypoxic conditions (1% O₂) for 24 h. NDUFA4L2 mRNA levels were quantified by real-time RT-PCR and they are expressed relative to normoxic RCC4/VHL. (C) Hif1α^{+/+}/Cre MEFs and Hif1α^{+/f}/Cre MEFs in the presence or absence of tamoxifen (1 μM) were cultured under normoxic or hypoxic conditions (1% O₂) for 18 h. NDUFA4L2 mRNA levels were quantified by real-time RT-PCR. (D) Schematic representation of the human NDUFA4L2 gene and the nucleotide sequences matching the consensus hypoxia-response element (HRE) from five mammalian genes, indicating the regions A-B-C analyzed in the ChIP assay. (E) ChIP assay of HIF-1α binding to the human NDUFA4L2 gene in HeLa cells cultured in normoxic or hypoxic conditions (1% O₂), or exposed to DMOG (0.1 mM) for 6 h. RT-PCR quantification of regions A (putative NDUFA4L2 HRE), B (non-conserved HRE) and C (negative HRE) after immunoprecipitation with HIF-1α

or a control antibody and represented as the percentage of that quantified in the total input DNA. (F) Representative gel of DNA amplified in the ChIP assays shown in panel E. See also Figure S2. (n>3; mean \pm SEM; *, p<0.05; **, p<0.01).

Figure 3. NDUFA4L2 decreases oxygen consumption, membrane potential and ROS production in hypoxia. HeLa cells were transfected with a scramble control or NDUFA4L2 siRNA and exposed to normoxic or hypoxic (1% O₂) conditions for 18-24 h. (A) Immunoblot analysis of NDUFA4L2 and HIF-1 α protein levels using tubulin and mitochondrial porin as loading controls. The images are representative of 4 independent experiments. (B) Oxygen consumption rates were measured by high-resolution respirometry. (C-D) HeLa cells were transfected with the empty vector (EV) or pCMV-NDUFA4L2 and then exposed to normoxic or hypoxic (1% O₂) conditions for 24 h. Immunoblot analysis of NDUFA4L2 and myc-tagged protein levels using tubulin and mitochondrial porin as loading controls (C). The images are representative of 4 independent experiments. (D) Oxygen consumption rates were measured by high-resolution respirometry. (E). Relative DCF fluorescence as a measure of intracellular hydrogen peroxide levels. (F) Representative images of 4 independent experiments showing MitoSOX intensity as a measure of mitochondrial superoxide levels. (G-H) Mitochondrial membrane potential was determined with the fluorescent probe TMRE and expressed relative to the control cells in normoxia. FCCP was used as a positive control of mitochondrial membrane depolarization (n>3; mean \pm SEM; *, p<0.05; **, p<0.01).

Figure 4. NDUFA4L2 decreases Complex I activity in hypoxia. (A-B) Complex I activity was measured in HeLa cells transfected with a scramble control or NDUFA4L2 siRNA (A), or with the empty or pCMV-NDUFA4L2 vector (B), then exposed to normoxic or hypoxic (1% O₂) conditions for 24 h. (C-D) Complex IV activity was measured in HeLa cells transfected with a scramble control or NDUFA4L2 siRNA (C), and the empty or pCMV-NDUFA4L2 vector (D), then exposed to normoxic or hypoxic (1% O₂) conditions for 24 h. (E-F) Complex I activity was measured in Hif1 $\alpha^{+/+}$ /Cre (E) or Hif1 $\alpha^{+/-}$ /Cre MEFs (F) maintained in the presence or absence of tamoxifen (1 μ M) for 48 h and cultured under normoxic or hypoxic (1% O₂) conditions for 18 h (G) Blue native PAGE (BN-PAGE) analysis of the mitochondrial OXPHOS Complex I (NDUFA9), Complex III (Core 2) and Complex IV (Col) from scramble and NDUFA4L2 siRNA HeLa cells exposed to normoxic or hypoxic (1% O₂) conditions for 24 h (n>3; mean \pm SEM; *, p<0.05; **, p<0.01).

Figure 5. Reduced hypoxic levels of NDUFA4L2 impair cell proliferation. (A-B) Growth curves of HeLa cells transfected with a scramble control or NDUFA4L2 siRNA in normoxic (A) and hypoxic (0.5% O₂) (B) conditions for different periods of time. (C) Microscope images showing the density of HeLa cell cultures transfected with a scramble control or NDUFA4L2 siRNA, and maintained under normoxic (21% O₂) or hypoxic (0.5% O₂) conditions for 72 h. (D) HeLa cells were transfected with either a scramble control or NDUFA4L2 siRNA and cultured under normoxic (21% O₂) or hypoxic (0.5% O₂) conditions for 72 h, and the cell lysates were assayed in immunoblots that were probed with antibodies against NDUFA4L2, uncleaved caspase-3 and cleaved caspase-3. Glut1 was used as a positive control of hypoxic gene induction and tubulin as a loading

control. Taxol was used as positive control of apoptosis. (E) Scramble control or NDUFA4L2 siRNA HeLa cells maintained in normoxic (21% O₂) or hypoxic (0.5% O₂) conditions for 72 h. The absolute value of apoptosis was measured by flow cytometry in cells stained with propidium iodide, as described in the experimental procedures. (F) Image of colony formation by HeLa cells transfected with a scramble control or NDUFA4L2 siRNA in normoxic and hypoxic (0.5% O₂) conditions in soft agar for 15 days. Both size and number of colonies were quantified (G) Growth of HeLa cells transfected with a scramble control or NDUFA4L2 siRNA in normoxic and hypoxic (0.5% O₂) conditions with or without 0.5 μ M MitoQ (0.5 μ M dTPP was used as control of MitoQ) at 72 h. (H) Fluorescence microscopy images of hypoxic (0.5% O₂) cultured scramble and siNDUFA4L2 HeLa cells and treated either with 0.5 μ M MitoQ or 0.5 μ M dTPP (n>3; mean \pm SEM; *, p<0.05; **, p<0.01).

Figure 6. Analysis of NDUFA4L2 deficient MEFs. WT and KO MEFs were exposed to 0,5% hypoxia 24h prior to subsequent analysis: (A) Immunoblot analysis showing the total deficiency of NDUFA4L2. Tubulin was used as a loading control. (B) Oxygen consumption rates were measured by high-resolution respirometry (Oxygraph 2k). Complex I (C) and Complex IV (D) activities were measured spectrophotometrically and expressed relative to citrate synthase values. (E) Relative growth rates of WT and KO NDUFA4L2 MEFs cultured in hypoxia (0.5% O₂). (F) Representative images of 3 independent experiments showing MitoSOX intensity as a measure of mitochondrial superoxide levels. (n>3 mean \pm SEM; *, p<0.05, **, p<0.01).

Figure 7. Opposite regulation of NDUFA4 and NDUFA4L2 under hypoxia. (A) HeLa cells were cultured under hypoxia (1% O₂) for 6, 12, 24 and 48 h and NDUFA4 mRNA levels were analyzed (B) Immunoblot analysis of HeLa cells subjected to either 24 h or 48 h of hypoxia and probed against NDUFA4, NDUFA4L2 antibodies. NDUFA9 was used as a loading control for Complex I and tubulin was used as a total loading control. (C) HeLa cells were transfected with a scramble control or NDUFA4L2 siRNA and then exposed to normoxic or hypoxic (1% O₂) conditions for 24 h, or transfected with the empty or pCMV-NDUFA4L2 vector (D). Cell lysates were analyzed against NDUFA4, NDUFA4L2 and tubulin antibodies. (E). Immunoblot analysis of MEF WT and KO for NDUFA4L2 showing the total deficiency of NDUFA4L2 and the decrease of NDUFA4 under hypoxic (1% O₂) conditions for 24 h. Tubulin was used as a loading control. (F) Model showing the involvement of NDUFA4L2 induction by HIF-1 α in hypoxic adaptation. HIF-1 α stabilization by hypoxia up-regulates NDUFA4L2, which inhibits ETC Complex I activity. As a result, oxygen consumption decreases and ROS production is abrogated, thereby allowing cells to adapt to the hypoxic conditions. In contrast, hypoxia decreases NDUFA4 protein levels. (n>3; mean \pm SEM; *, p<0.05; **, p<0.01).

Figure1

Fig.1. Tello *et al*

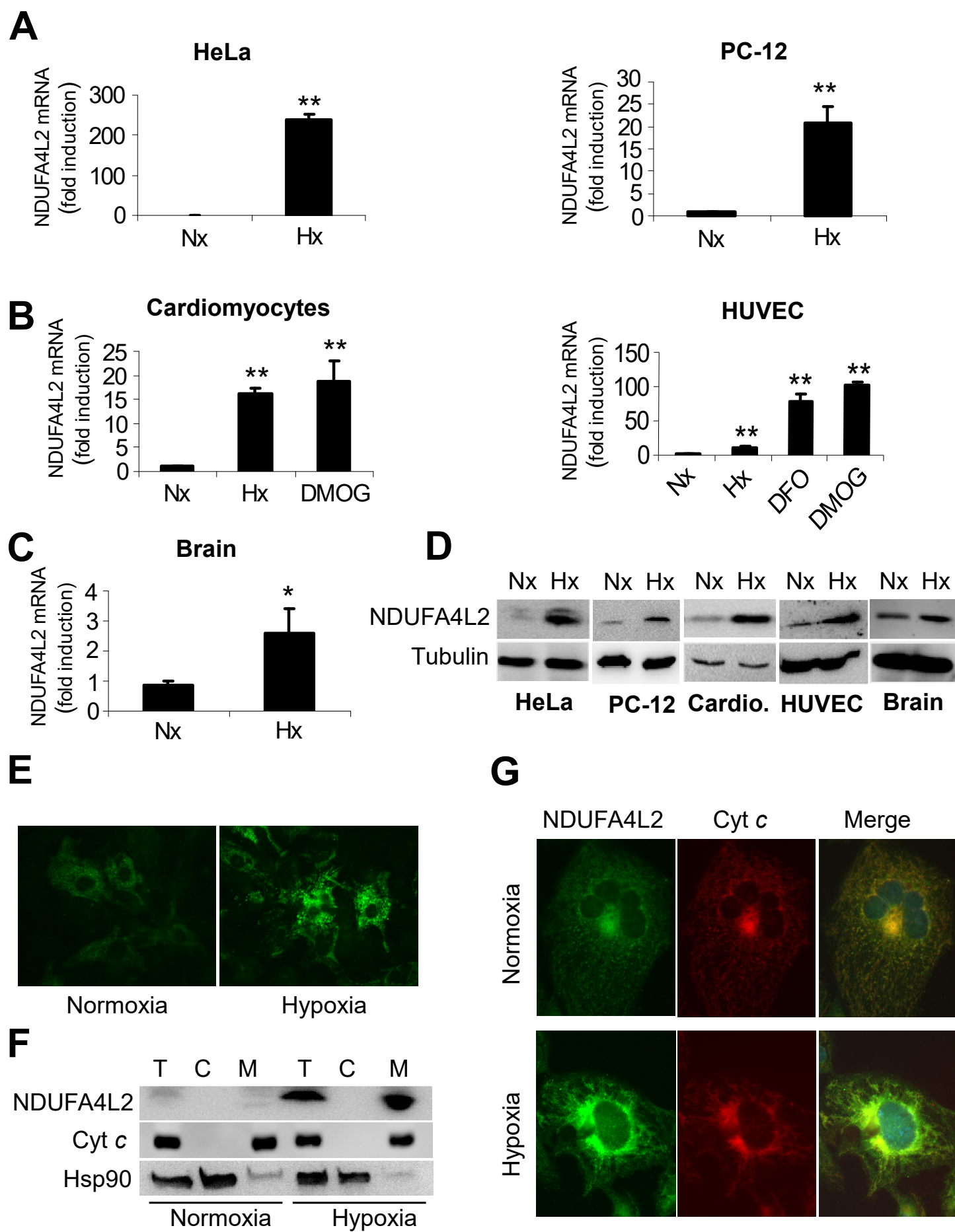


Figure2

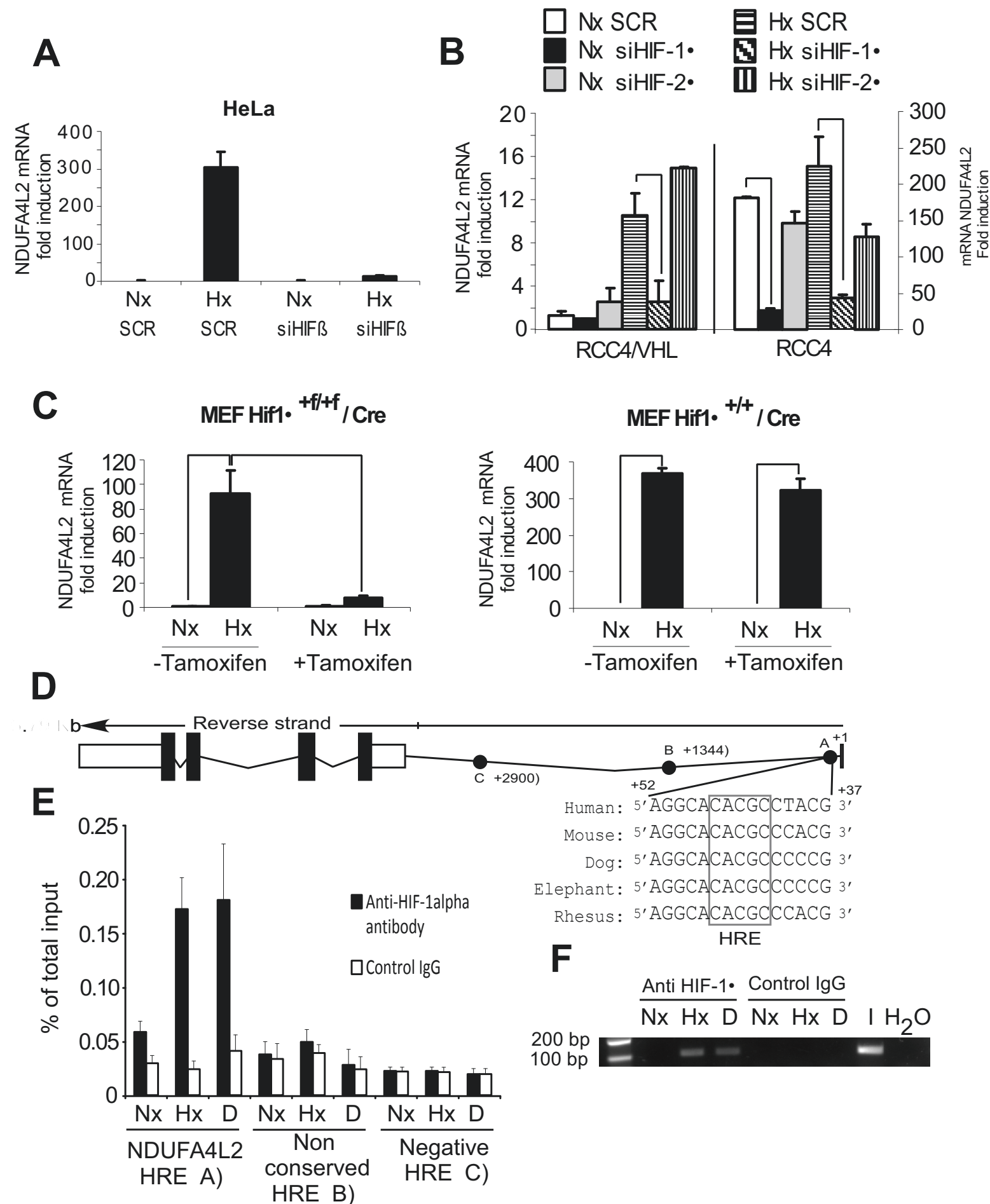
Fig.2. Tello *et al*

Figure3

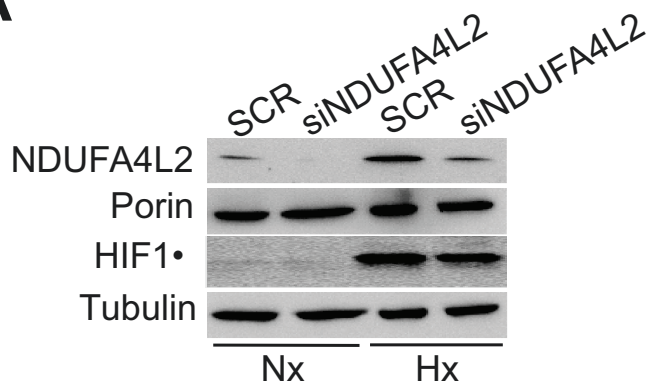
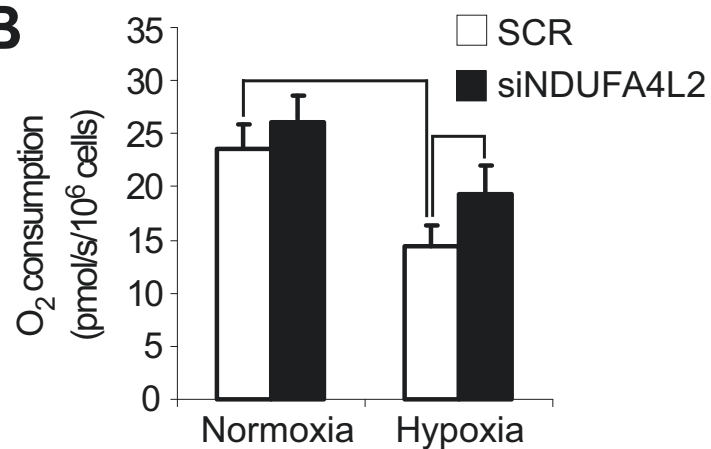
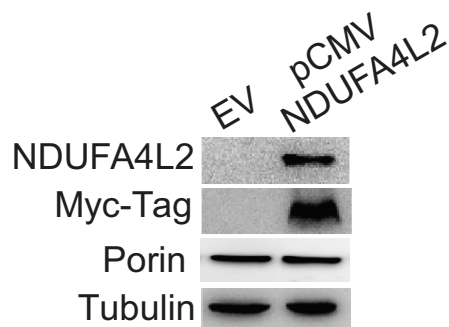
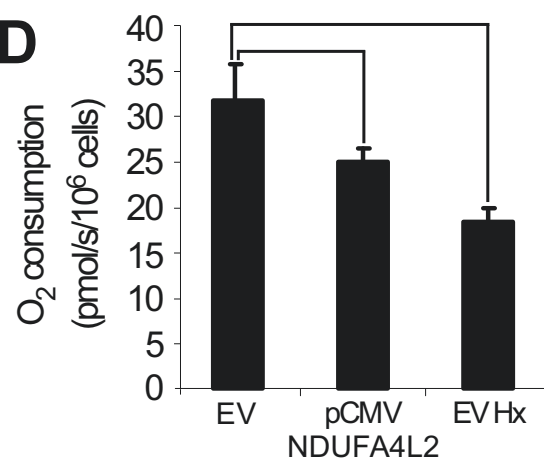
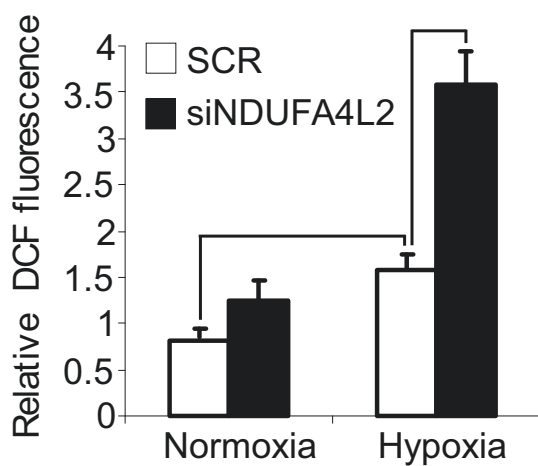
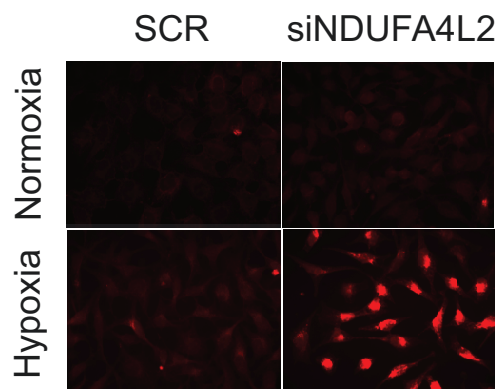
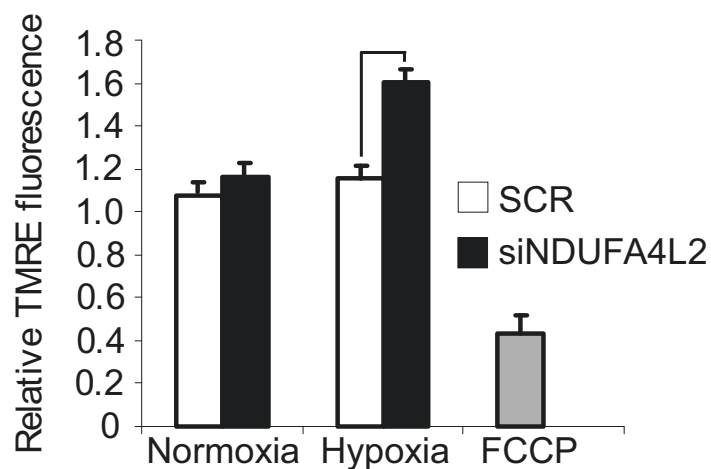
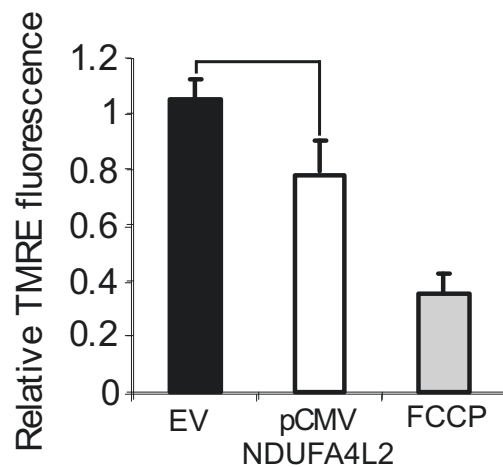
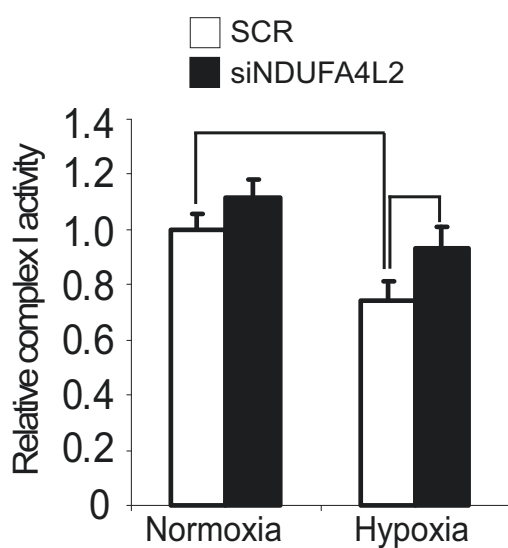
Fig.3. Tello *et al***A****B****C****D****E****F****G****H**

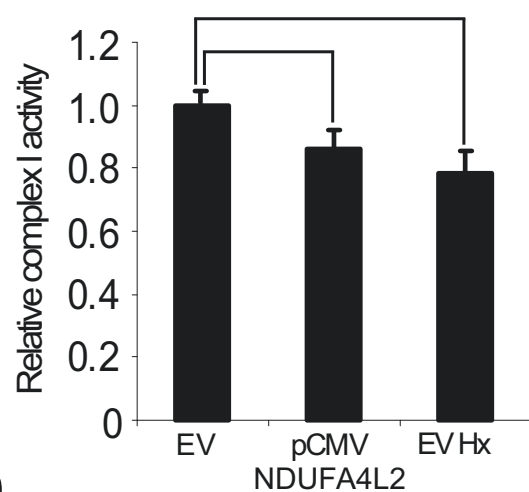
Figure4

Fig.4. Tello *et al*

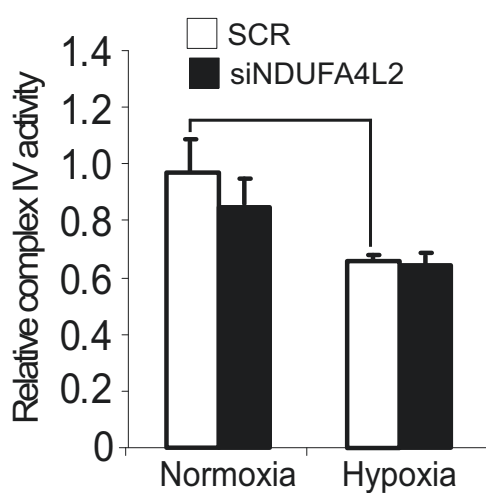
A



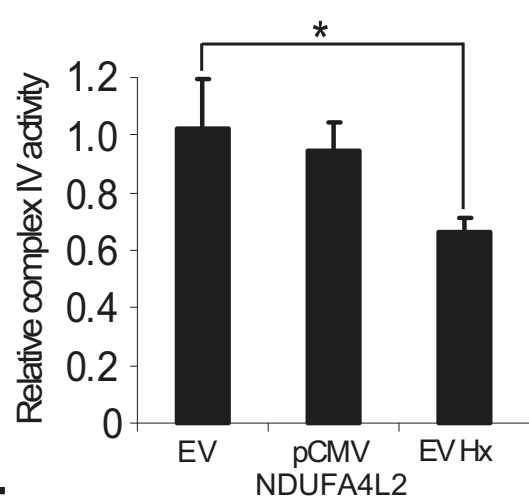
B



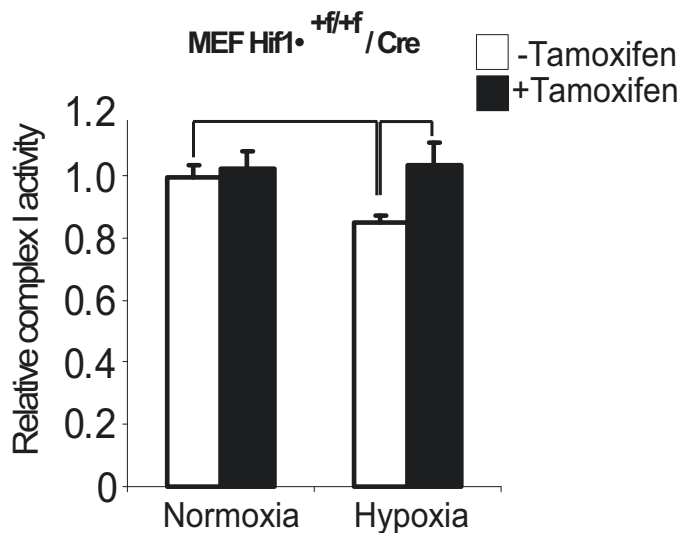
C



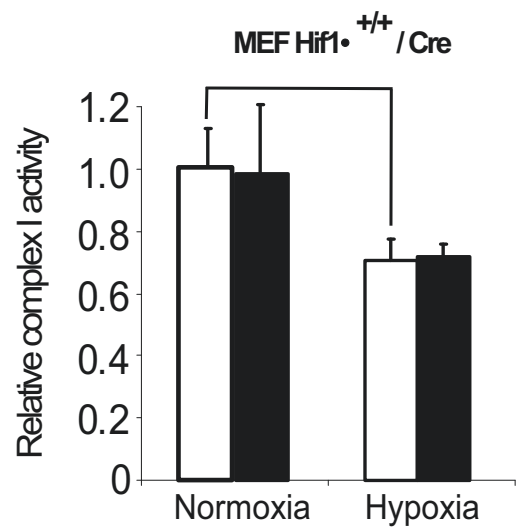
D



E



F



G

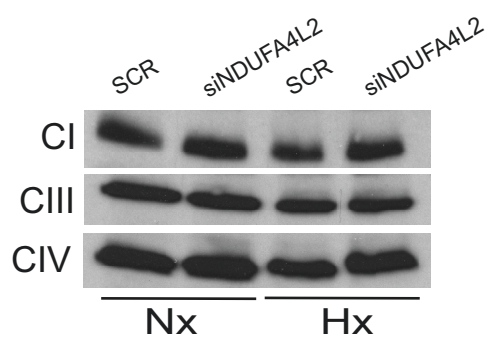


Figure 5

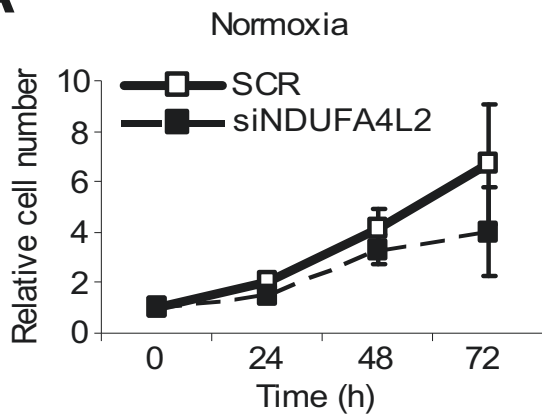
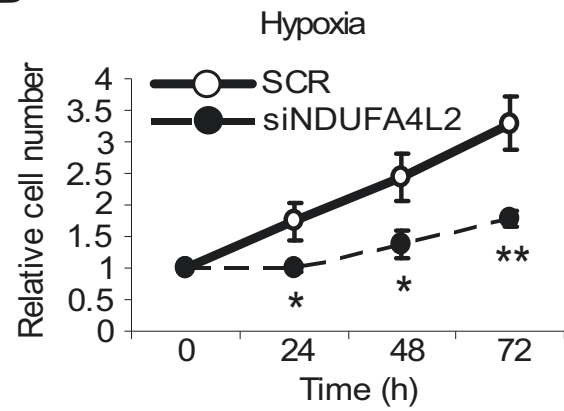
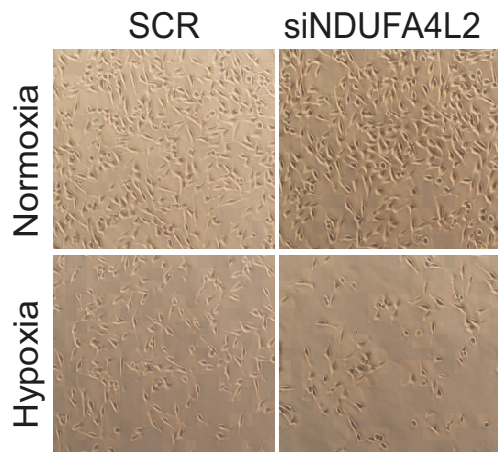
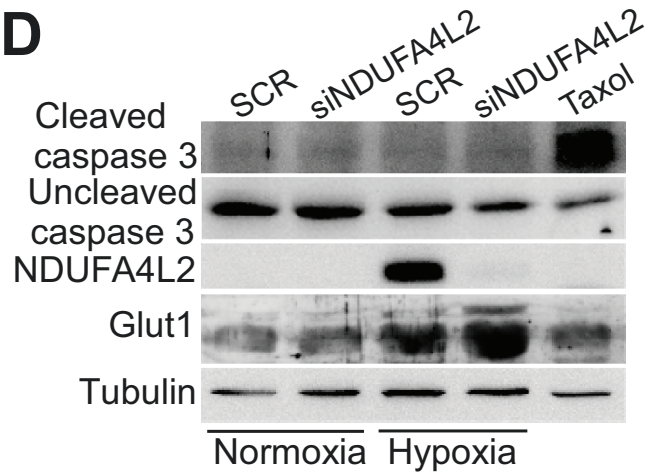
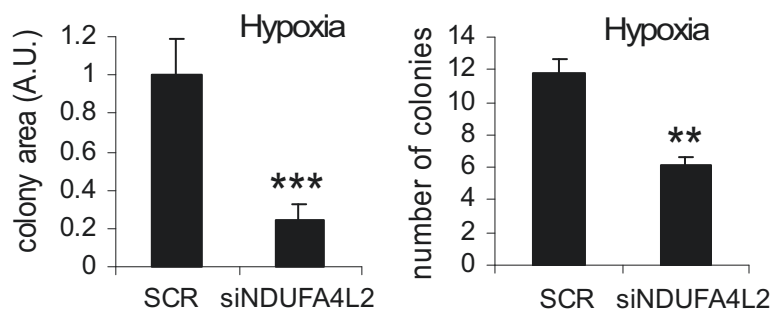
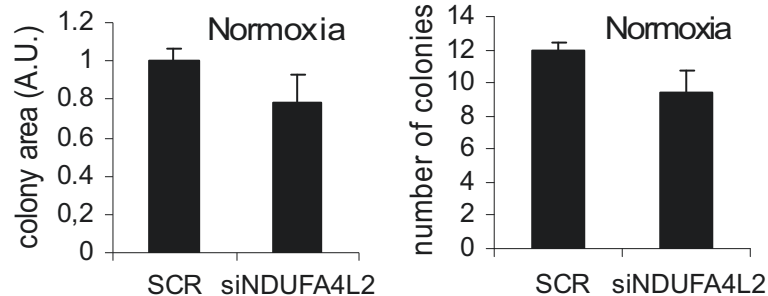
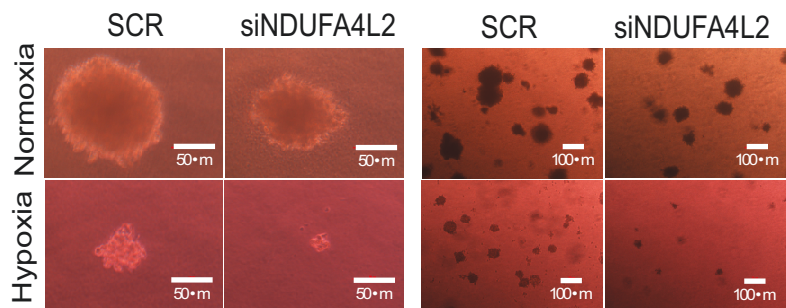
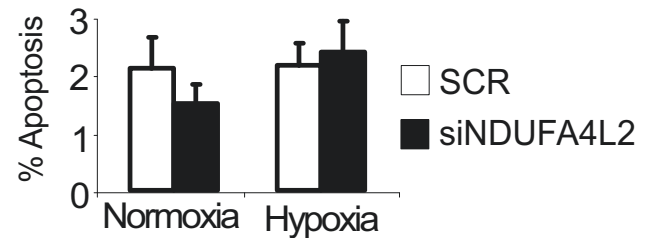
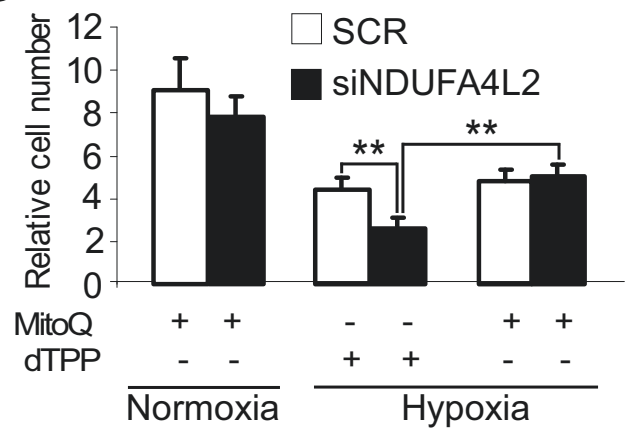
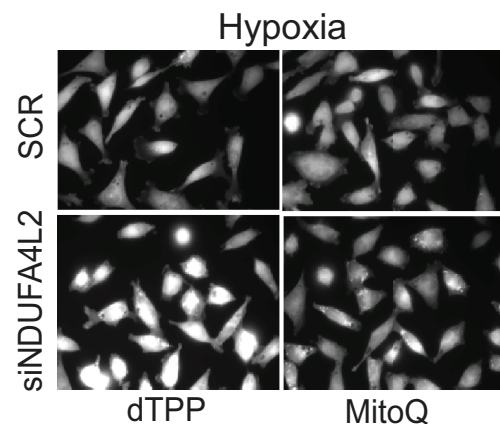
Fig.5. Tello *et al***A****B****C****D****F****E****G****H**

Figure6
Fig.6. Tello *et al*

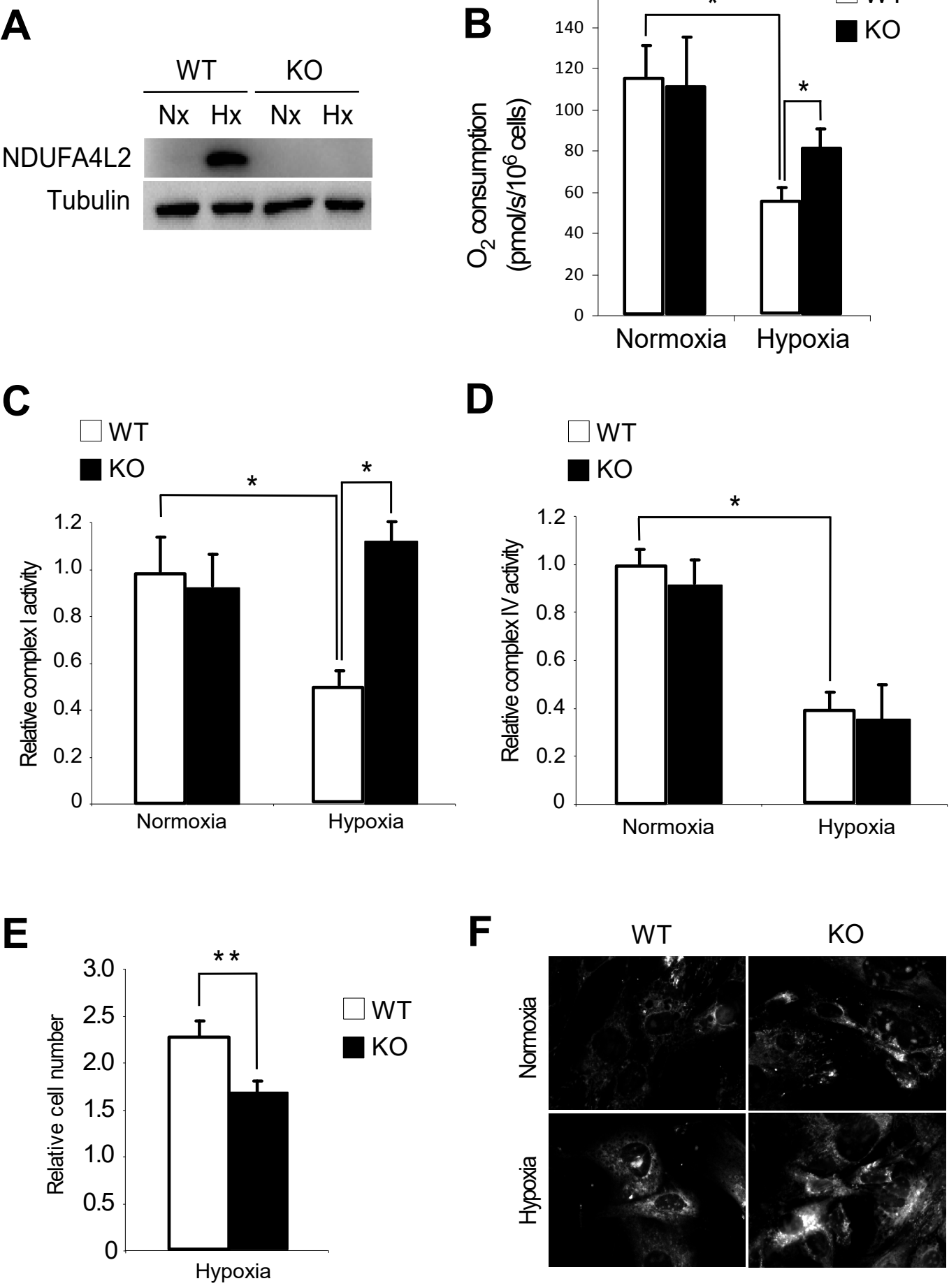
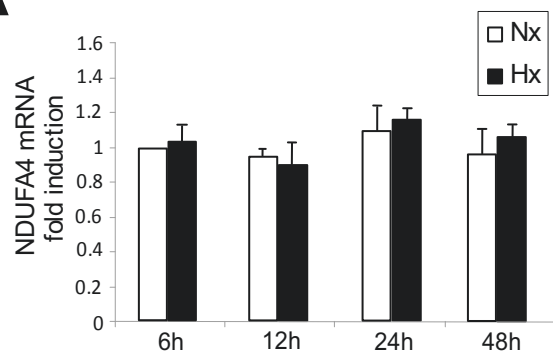
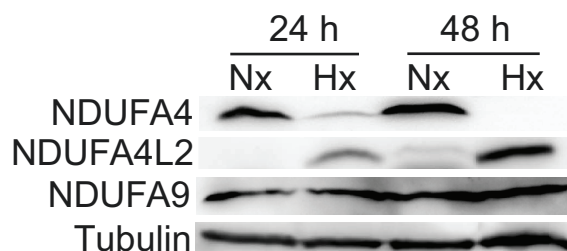


Fig.7. Tello *et al*

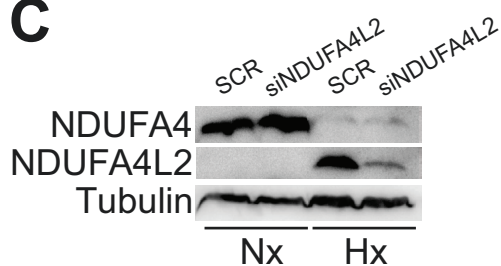
A



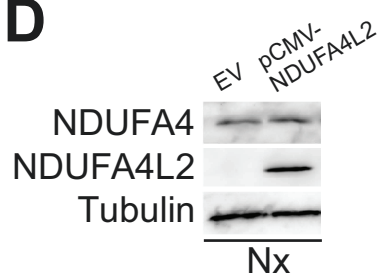
B



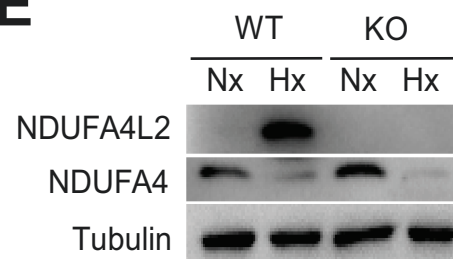
C



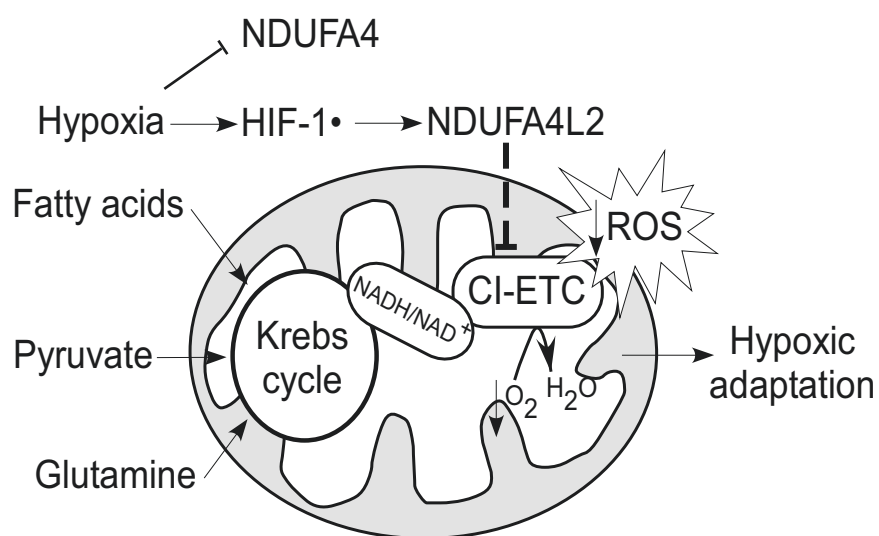
D



E



F



Supplemental information

**Induction of the mitochondrial NDUF4L2 protein by HIF1 α
decreases oxygen consumption by inhibiting Complex I activity**

Supplemental Figures and Legends

Figure S1. Related to Figure 1

Supplemental Data

Figure S1

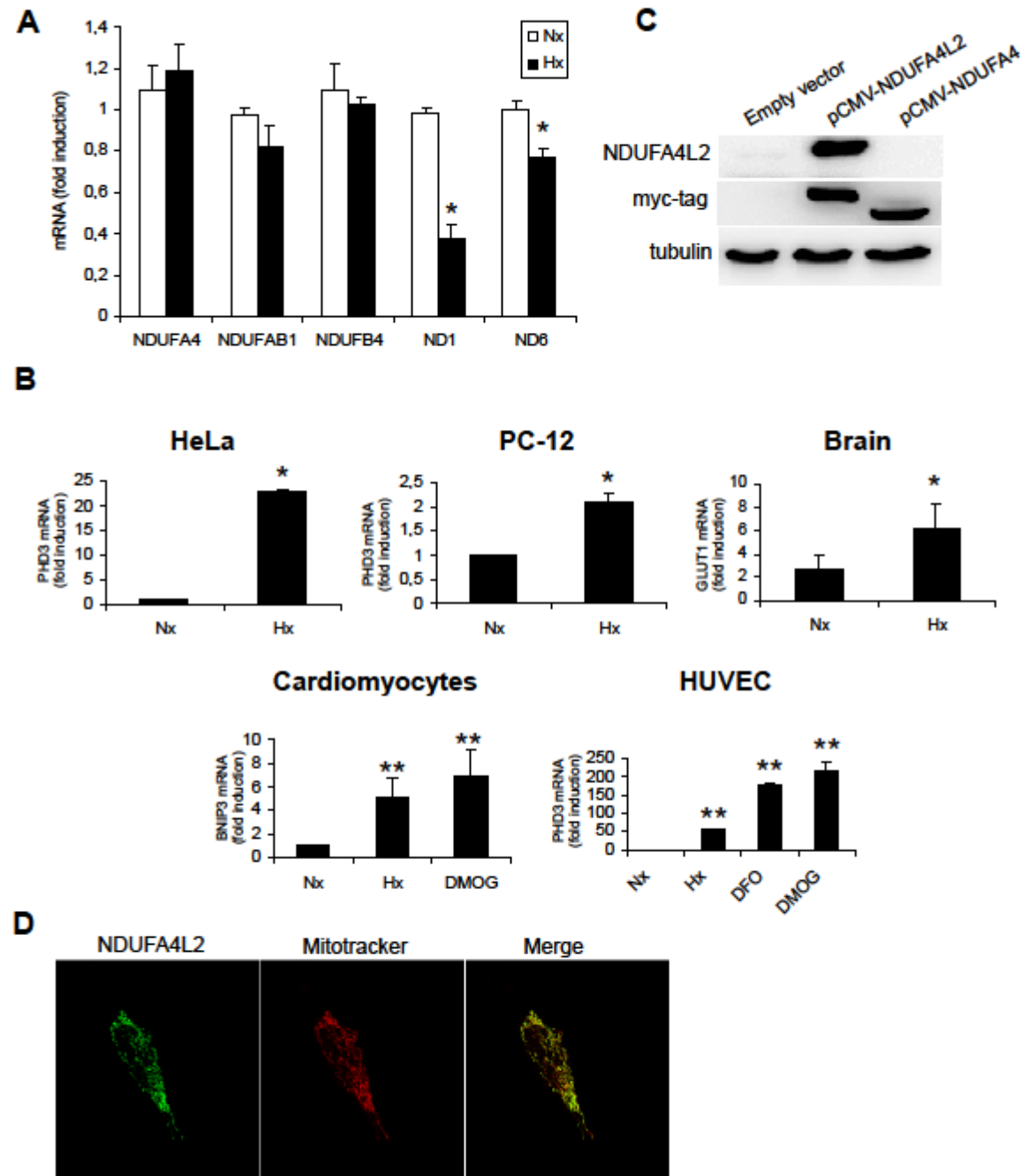


Figure S2. Related to Figure 2

Figure S2

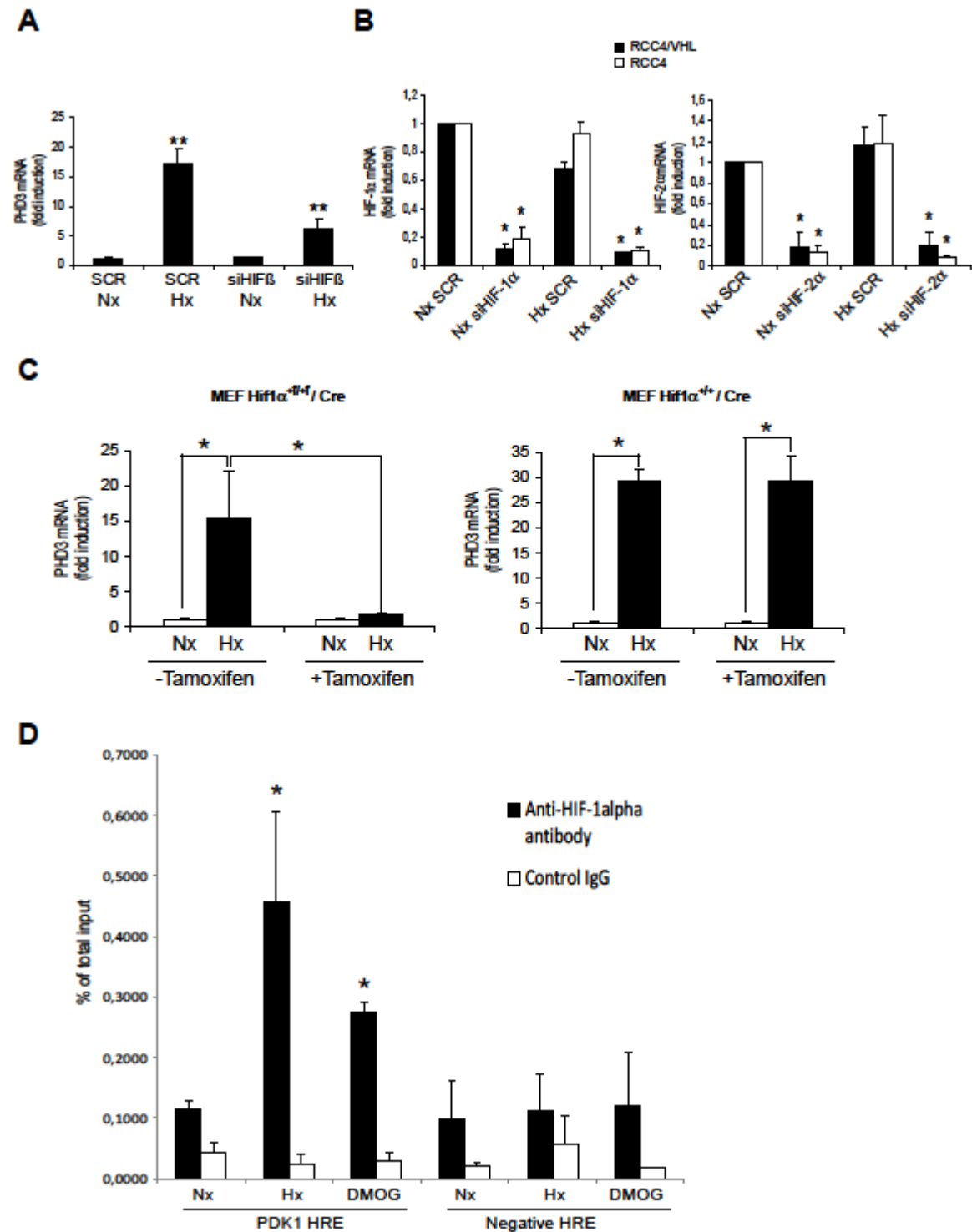


Figure S3. Related to Figure 3 and 4

Figure S3

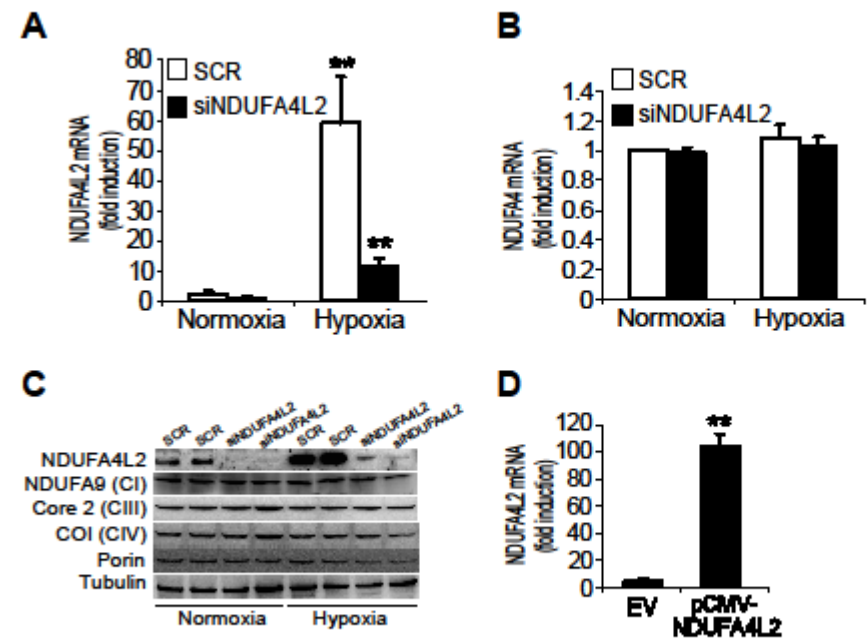


Figure S4. Related to Figure 5

Figure S4

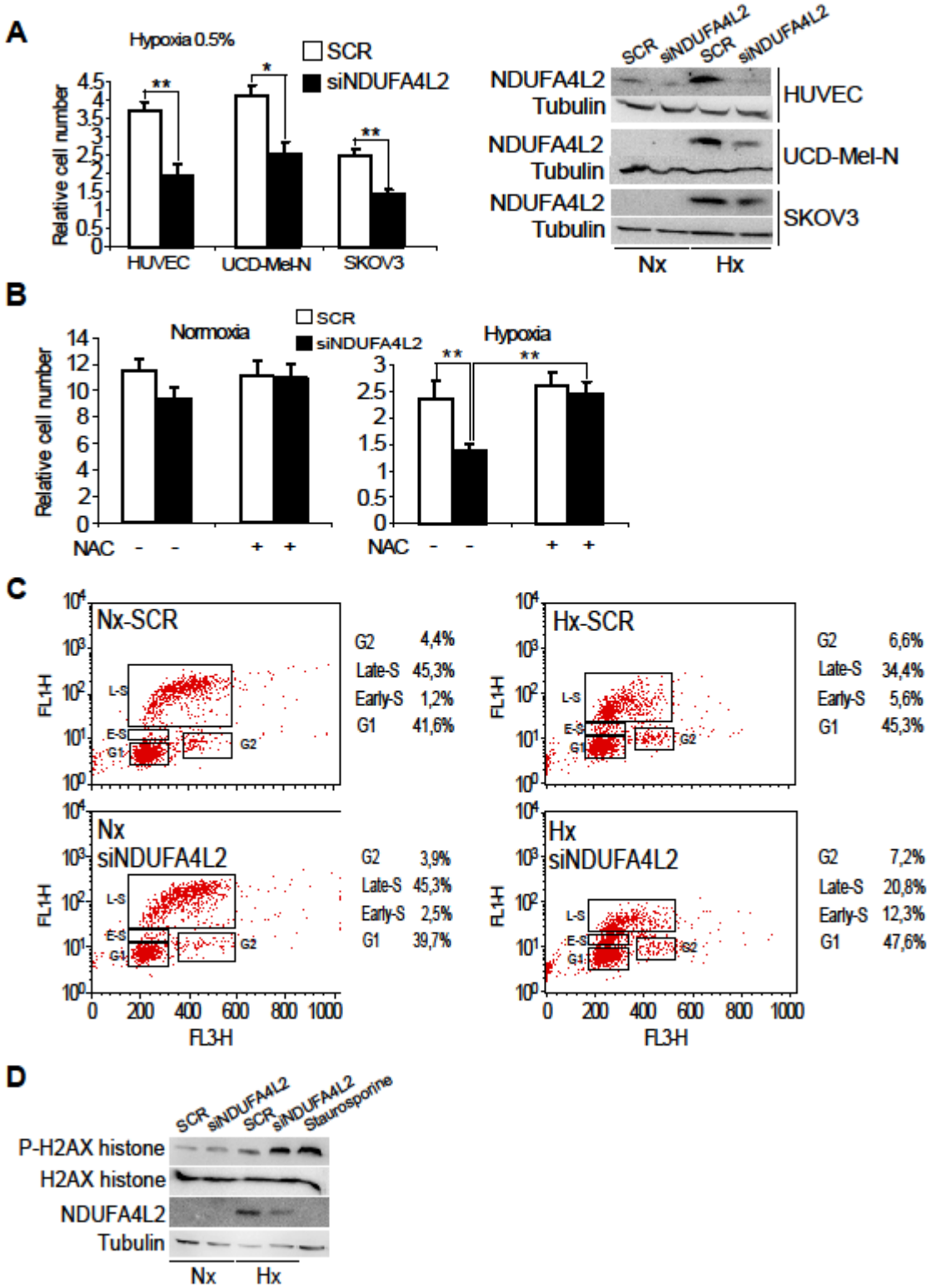
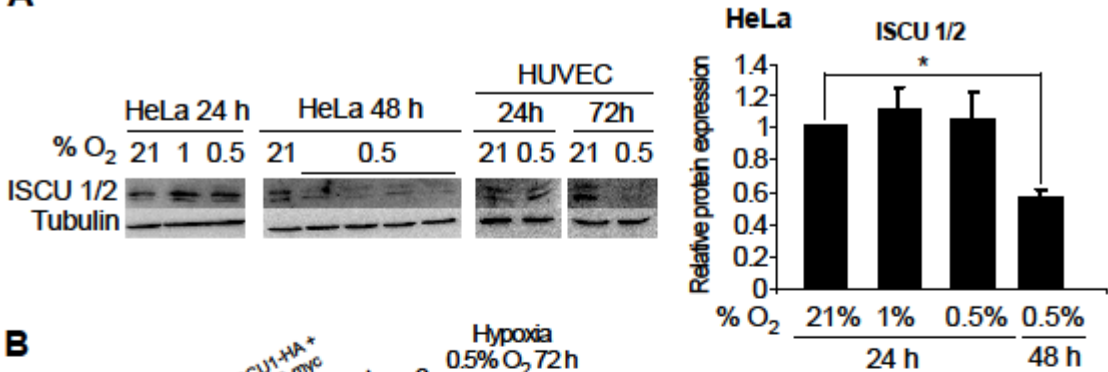


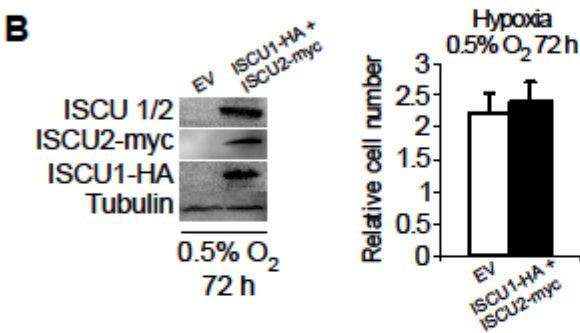
Figure S5. Related to Figure 4

Figure S5

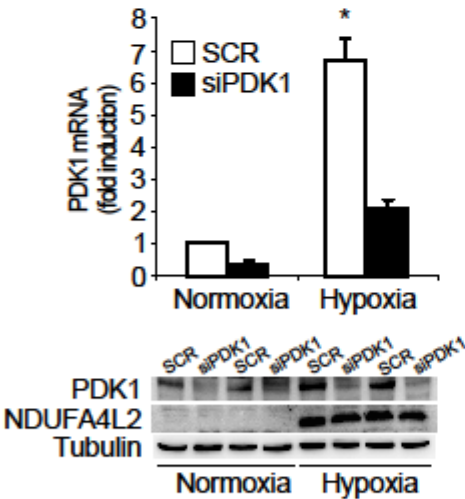
A



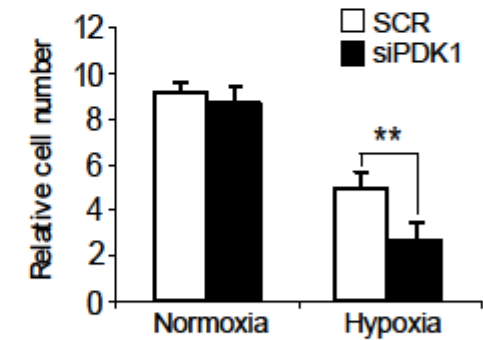
B



C



D



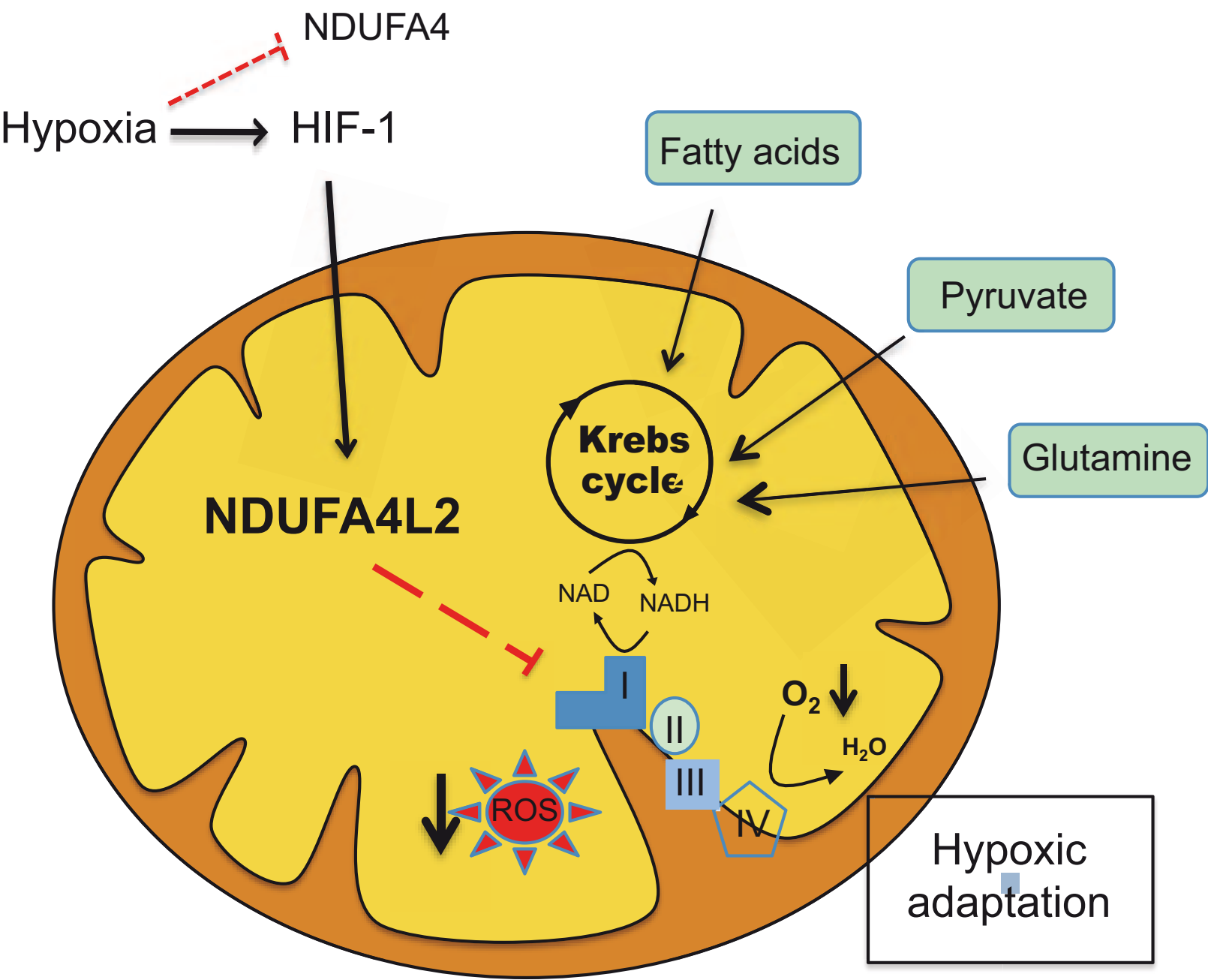


Figure S1. (A) Quantitative RT-PCR analysis of nuclear and mitochondrial gene expression in HeLa cells cultured under normoxic or hypoxic (1% O₂) conditions for 6 h. The levels of NDUFA4, NDUFB1, NDUFB4, ND1 and ND6 were determined by quantitative RT-PCR. (B) Quantitative RT-PCR analysis of known HIF-1 α target genes (*PHD3*, *GLUT1* and *BNIP3*) as positive controls for hypoxic gene induction in HeLa, PC-12, cardiomyocytes, HUVEC and brain tissue. Hypoxic conditions are as stated in Figure 1. (C) Immunoblot showing the specificity of the NDUFA4L2 antibody. HeLa cells were transfected with the empty vector, pCMV-NDUFA4L2 or pCMV-NDUFA4, and the protein extracts were probed with antibodies against NDUFA4L2, myc-tag and tubulin as a loading control. The image shown is representative of 3 experiments. (D) Confocal immunofluorescence of HeLa cells treated with either FITC goat anti-rabbit IgG to verify the presence of NDUFA4L2 (left panel, green) or mitotracker, a mitochondrial marker (middle panel, red). The right panel is an overlay of the two signals and the images shown are representative of 3 experiments. (n>3; mean \pm SEM; *, p<0.05; **, p<0.01).

Figure S2. (A) HeLa cells were transfected with a siRNA against HIF β or a scrambled control and 24 h after transfection, the cells were seeded again and cultured under normoxic or hypoxic (1% O₂) conditions for a further 24 h. PHD3 mRNA levels were quantified by real-time RT-PCR. (B) VHL-deficient RCC4 cells or RCC4/VHL cells were transfected with a siRNA against HIF-1 α , HIF-2 α or a scrambled control. After transfection (24 h), the cells were seeded again and cultured under normoxic or hypoxic (1% O₂) conditions for a further 24h. HIF-1 α and HIF-2 α mRNA levels were quantified by real-time RT-PCR. (C)

Hif1 α ^{+/+}/Cre and Hif1 α ^{+/f}/Cre MEFs were maintained in the presence or absence of tamoxifen (1 μ M) and cultured under normoxic or hypoxic (1% O₂) conditions for 18h. The PHD3 mRNA levels were quantified by real-time RT-PCR. (D) Chromatin immunoprecipitation assay of HIF-1 α binding to the human PDK1 gene. The RT-PCR quantification of regions including PDK1 HRE (A) and a negative HRE (B) is indicated as the percentage of that in the total input chromatin DNA. (n>3; mean \pm SEM; *, p<0.05; **, p<0.01).

Figure S3. (A) Quantitative RT-PCR analysis of NDUFA4L2 mRNA levels and (B) NDUFA4mRNA levels in HeLa cells transfected with a scrambled control or NDUFA4L2 siRNA followed by exposure to normoxic or hypoxic (1% O₂) conditions for 24 h. (C) Scramble and siNDUFA4L2 HeLa cells were submitted to hypoxia 24h, (1% O₂) , and cell lysate were analyzed by western blot to measure electron transport chain complexes protein levels. NDUFA9 for complex I, Core 2 for complex III and COI for complex IV. Antibody against Porin and Tubulin was used as a loading control. (D) Quantitative RT-PCR analysis of NDUFA4L2 mRNA levels in HeLa transfected either with empty vector (EV) or pCMV-NDUFA4L2. . (n>3; mean \pm SEM; **, p<0.01).

Figure S4 (A) Growth of HUVEC, UCD-Mel-N and SKOV3 cells transfected with a scramble control or NDUFA4L2 siRNA in hypoxic (0.5% O₂) conditions at 72 h. (B) Growth of HeLa cells transfected with a scramble control or NDUFA4L2 siRNA under hypoxia (0.5% O₂) with or without 0.1 mM N-acetylcysteine (NAC) 72 h. (C) Cell cycle analysis of HeLa cells transfected with a scramble control or NDUFA4L2 siRNA in normoxia and hypoxia (0.5% O₂) at 24 h. (D) H2AX histone phosphorylation analysis in HeLa cells transfected with a scramble

control or NDUFA4L2 siRNA in normoxic and hypoxic conditions (0.5% O₂) at 24 h (n>3; mean ± SEM; *, p<0.05; **, p<0.01).

Figure S5. (A) ISCU 1/2 protein expression in HeLa and HUVEC cells exposed under normoxic or hypoxic (1% or 0.5%) conditions at indicated times. (B) Growth of HeLa cells transfected with an empty vector (EV) or an expression vector encoding the ORF of ISCU1 with a 3' hemagglutinin (HA) tag (ISCU1-HA) and an expression vector encoding the ORF of ISCU2 with a 3' myc epitope (MYC) tag (ISCU2-myc) under hypoxia (0.5% O₂) at 72 h. (C). Quantitative RT-PCR and immunoblot analysis of PDK1 mRNA and protein levels in HeLa cells transfected with a scramble control or PDK1 siRNA followed by exposure to normoxic or hypoxic (0.5% O₂) conditions for 72 h. (D) Growth of HeLa cells transfected with a scramble control or PDK1 siRNA in normoxic and hypoxic (0.5% O₂) conditions at 72h. (n>3; mean ± SEM; *, p<0.05; **, p<0.01).

Supplemental Tables

Table S1 - List of Complex I genes and hypoxia-induced expression obtained in our mRNA array study performed in HeLa cells

Gene symbol	Identifier	Average fold change	Gene symbol	Identifier	Average fold change
NDUFA4L2	NM_020142	9.95	NDUFA3	NM_004542	0.01
NDUFA1	NM_004541	0.26	NDUFB2	NM_004546	0.00
NDUFB5	NM_002492	0.23	NDUFB1	NM_004545	-0.00
NDUFA6	NM_002490	0.22	NDUFS8	NM_002496	-0.01
NDUFB8	NM_005004	0.21	NDUFA12	NM_018838	-0.01
NDUFC1	NM_002494	0.20	NDUFA5	NM_005000	-0.01
NDUFS4	NM_002495	0.19	NDUFS3	NM_004551	-0.03
NDUFV1	NM_007103	0.15	NDUFA8	NM_014222	-0.03
NDUFA7	NM_005001	0.14	NDUFA2	NM_002488	-0.06
NDUFB6	NM_182739	0.14	NDUFA11	NM_175614	-0.06
NDUFS2	NM_004550	0.14	NDUFB10	NM_004548	-0.06
NDUFB11	NM_019056	0.12	NDUFS5	NM_004552	-0.08
NDUFA12L	NM_174889	0.11	NDUFV2	NM_021074	-0.09
NDUFA4	NM_002489	0.10	NDUFB3	NM_002491	-0.09
NDUFS1	NM_005006	0.07	NDUFC2	NM_004549	-0.11
NDUFB4	NM_004547	0.06	NDUFAB1	NM_005003	-0.11
NDUFB7	NM_004146	0.06	NDUFAF1	NM_016013	-0.12
NDUFA9	NM_005002	0.05	NDUFV3	NM_021075	-0.12
NDUFS6	NM_004553	0.05	ND2	ENST00000361453	-0.76
NDUFB9	NM_005005	0.04	ND3	ENST00000361227	-1.92
NDUFA10	NM_004544	0.03	ND1	ENST00000361390	-2.72
NDUFS7	NM_024407	0.01	ND6	ENST00000361681	-2.79
NDUFA13	NM_015965	0.01			

Table S2. Genes expressed more strongly in hypoxic conditions in our mRNA array study on HeLa cells

Position	Gene symbol	Identifier	average fold increase
1	EDN2	NM_001956	12.37
2	ANGPTL4	NM_139314	12.05
3	A_23_P170719	A_23_P170719	11.92
4	GAL3ST1	NM_004861	10.98
5	IGFBP3	NM_001013398	10.88
6	THC2585656	THC2585656	10.40
7	HLXB9	NM_005515	10.32
8	THC2585656	THC2585656	10.26
9	LOC283666	BC048264	10.12
10	ZP1	NM_207341	9.98
11	NDUFA4L2	NM_020142	9.95
12	IGFBP3	NM_001013398	9.46

Table S3. Predicted subcellular location of NDUFA4L2

Program	URL	Predicted localization
HSLpred	http://www.imtech.res.in/raghava/hslpred/	Mitochondria
ProtComp V6.0	http://www.softberry.com	Mitochondria
MitoProt II - v1.101	http://www.med.tu-muenchen.de/	Mitochondria

Table S4. Primer sequences for RT-PCR analysis.

Gene	Sequence	
	Forward	Reverse
hNDUFA4L2	5'- TTCTACCGGCAGATCAAAAGACA - 3'	5'- GGGCGAGTCGCAGCAA - 3'
mNDUFA4L2	5'- CCTGCGCAGTCCTGATGTCT - 3'	5'- GGTTGAAACGGCAAGGAAGCTT - 3'
rNDUFA4L2	5'- CCGCTTCTACCGGCAGATAA - 3'	5'- CCATGCCCAAGCAGATGAA - 3'
hNDUFA4	5'- TCGTCTGGCATTGTTCAA - 3'	5'- TCCAGGGCTCTGGGTATTTC - 3'
hNDUFAB1	5'- TTGCAGCCGGCCTTAGTG - 3'	5'- CTCTAACGTCAAAGGAGGCATGT - 3'
hNDUFAB4	5'- GCCATAAGAGCCCAGCTGAA - 3'	5'- ACGAAGCAAGGCAGGATTTTC - 3'
hND1	5'- CCCTTCGCTGACGCCATA - 3'	5'- TGGTAGATGTGGCGGCGGGTTTT - 3'
hND6	5'- GGGTTAGCGATGGAGGTAGGA - 3'	5'- CAACCACCACCCCATCATACT - 3'
hPHD3	5'- GCCGGCTGGGCAAATACTA - 3'	5'- CCGGATAGCAAGCCACCAT - 3'
mPHD3	5'- TGGACAACCCCAATGGTGAT - 3'	5'- GCAGGACCCCTCCATGTAAGT - 3'
h/rBNIP3	5'- GTCTGGACGGAGTAGC - 3'	5'- GGCCGACTTGACCAAT - 3'
rGLUT1	5'- CGCAACGAGGAGAACC - 3'	5'- GCCGTGTTGACGATACC - 3'
hHIF-1 α	5'- GTTTACTAAAGGACAAGTCAC - 3'	5'- TTCTGTTTGTGAAGGGAG - 3'
hEPAS	5'- CAATCAGCTTCCTGCGAACA - 3'	5'- TTCGGCTTCGGACTCGTTT - 3'
m/rHPRT	5'- GTTAAGCAGTACAGCCCCAAA - 3'	5'- AGGGCATATCCAACAACAACTT - 3'
hHPRT	5'- ATTGTAATGACCAGTCAACAGGG - 3'	5'- GCATTGTTTGGCAGTGTCAA - 3'
hPDK1	5'- GTGGTTTATGTACCATCCCATCTCT - 3'	5'- TCCATAGTGGCTCTCATTGCAT - 3'

Table S5. Primer sequences for CHIP assays

Gene	Region	Sequence	
		Forward	Reverse
hNDUFA4L2	A	5'- CAGGTCTGTGTATGTGTGAAA - 3'	5'- CTACGCACTGTCACTGAG - 3'
hNDUFA4L2	B	5'- GGTGTATGTTAATCATGGCTCAG - 3'	5'- CAGCCAGAGGAAGTGGA - 3'
hNDUFA4L2	C	5'- CGCTAAGTTGGTGCCTG - 3'	5'- CGATTGTGGCTGGAGAGATA - 3'
hPDK1	HRE (A)	5'- CGCGTTTGGATTCCGTG - 3'	5'- CCAGTTATAATCTGCCTTCCCTATTATC - 3'
hPDK1	Non-HRE (B)	5'- AAAGGACATTCTACAACGATTCTGC - 3'	5'- CAATTGTCTGGTTACTGAAAGTCTCC - 3'

Supplemental Experimental Procedures

Cell lines and cell cultures. HeLa, SKOV3, UCD-mel-N, RCC4, RCC4/VHL, neonatal rat cardiomyocytes and Hif1 $\alpha^{+/+}$ /Cre or Hif1 $\alpha^{+f/+f}$ /Cre mouse embryo fibroblasts (MEFs) were cultured in DMEM containing 10% heat-inactivated fetal bovine serum (FBS). PC-12 cells were cultured in RPMI containing 10% heat-inactivated fetal horse serum and 5% FBS. Human umbilical vein endothelial cells (HUVEC) were cultured in 199 medium with 20% FBS and 1% ECGF. HL-1 cells were cultured in Claycomb medium containing 10% heat-inactivated FBS and supplemented with 0.1 mM norepinephrine and 2 mM glutamax. All media were also supplemented with 100 IU/ml penicillin, 100 μ g/ml streptomycin and 1% HEPES buffer. Normoxic cells (21% O₂) were maintained at 37°C in a 5% CO₂/95% air incubator. For hypoxic exposure, cell culture dishes were placed into an Invivo₂ 400 humidified hypoxia workstation (Ruskin Technologies, Bridgend, UK) at 0.5% or 1% O₂. All other reagents were provided by Sigma (DFX) and Enzo (DMOG).

Quantitative RT-PCR. Total RNA extraction, cDNA synthesis, and qRT-PCR were carried out as described previously (Acosta-Iborra et al., 2009). Primer sequences are listed in *Table S4*.

ChIP assay. Chromatin immunoprecipitation and real-time PCR quantification were performed as described previously (Ortiz-Barahona et al., 2010). Primer sequences for the ChIP assay are shown in *Table S5*.

Plasmids and siRNAs. For transient overexpression, the pCMV-NDUFA4L2 and the pCMV-NDUFA4 myc-tagged open reading frame (ORF) human plasmids were purchased from Origene (Rockville, MD). An expression vector encoding the ORF of ISCU1 with a 3' hemagglutinin (HA) tag (ISCU1-HA) and an expression vector encoding the ORF of ISCU2 with a 3' myc epitope (MYC) tag (ISCU2-myc) (Tong and Rouault, 2000) were kindly provided by Stephen Y. Chan and Joseph Loscalzo. Plasmid transfection of HeLa cells was performed with lipofectamine 2000 (Invitrogen, Carlsbad, CA) according to the manufacturer's instructions. For knockdown experiments, human HIF-1 β siRNA (J-007207) and human PDK1 siRNA (J-054066) were purchased from Dharmacon, human HIF-1 α siRNA (sc-44225) and human NDUFA4L2 siRNA (sc-95677) were purchased from Santa Cruz Biotechnology, and human the HIF-2 α siRNA (5'-CAGCAUCUUUGAUAGCAG-3') was provided by Eurogentec. HeLa cells were transfected with siRNAs using the lipofectamine RNAiMAX reagent (Invitrogen, Carlsbad, CA) according to the manufacturer's instructions.

Western blot analysis. For use in standard polyacrylamide gel electrophoresis and immunoblotting, primary antibodies included polyclonal anti-NDUFA4L2 antibodies (Abcam or Proteintech), monoclonal anti-NDUFA9 antibody (Santa Cruz), monoclonal anti-Complex III subunit Core 2 antibody (Mitosciences), monoclonal anti-Complex IV subunit I antibody (Mitosciences), monoclonal anti-HIF-1 α antibody (Santa Cruz), monoclonal anti-cytochrome c antibody (BD), monoclonal anti-porin antibody (Invitrogen), monoclonal anti-Hsp90 antibody (Santa Cruz), polyclonal anti-total Caspase-3 antibody (Cell Signaling),

polyclonal anti-PDK1 antibody (Cell Signaling), polyclonal anti-IscU 1/2 antibody (Santa Cruz), monoclonal anti-myc antibody (Sigma), polyclonal anti-HA antibody (Santa Cruz), monoclonal anti-phospho H2AX antibody (Millipore), polyclonal anti-total H2AX antibody (Millipore) and monoclonal anti-tubulin antibody (Sigma) were used. Antibody binding was detected by enhanced chemiluminescence (ECL, Amersham Biosciences) with species-specific secondary antibodies labeled with Horseradish Peroxidase (HRP) (Dako, Amersham) and visualized on a digital luminescent image analyzer (Fujifilm LAS-1000 CH).

Immunofluorescence microscopy. After specific treatment, HeLa and HL-1 cells were grown on glass coverslips in 24-well culture dishes, fixed with 3% paraformaldehyde in HBSS for 15 min at room temperature, and washed with PBS. The cells were then permeabilized with 0.5% Triton X-100 for 10 min, and non-specific binding sites were blocked by incubation with 3% BSA in PBS for 30 min. The cells were incubated with the polyclonal anti-NDUFA4L2 antiserum (Abcam) or monoclonal anti-cytochrome c (BD) for 1 h at room temperature and then washed with PBS. A secondary Alexa 488 conjugated anti-rabbit antibody (Invitrogen) and the specific mitochondrial marker Mitotraker (Invitrogen) or Alexa 568 conjugated anti-mouse (Invitrogen) were then added to the cells for 30 min, before they were finally washed with PBS, washed briefly with distilled water, and mounted with Mowiol.

ROS measurements. Intracellular H₂O₂ and superoxide ion production were measured by staining HeLa cells with dichlorodihydrofluorescein diacetate (H₂DCFDA, Molecular Probes) and MitoSOX (Molecular Probes), respectively.

DCF fluorescence was measured using a FACScan flow cytometer, while MitoSOX fluorescence was observed by fluorescence microscopy (Redondo-Horcajo et al., 2010).

Cell cycle analysis. Cell cycle was analyzed using the Click-IT EdU Flow Cytometry Assay Kit according to the manufacturer's instructions.

References

Acosta-Iborra, B., Elorza, A., Olazabal, I.M., Martin-Cofreces, N.B., Martin-Puig, S., Miro, M., Calzada, M.J., Aragoes, J., Sanchez-Madrid, F., and Landazuri, M.O. (2009). Macrophage oxygen sensing modulates antigen presentation and phagocytic functions involving IFN-gamma production through the HIF-1 alpha transcription factor. *J Immunol* 182, 3155-3164.

Ortiz-Barahona, A., Villar, D., Pescador, N., Amigo, J., and Del Peso, L. (2010). Genome-wide identification of hypoxia-inducible factor binding sites and target genes by a probabilistic model integrating transcription-profiling data and in silico binding site prediction. *Nucleic Acids Res*, doi:10.1093/nar/gkp1205

Redondo-Horcajo, M., Romero, N., Martinez-Acedo, P., Martinez-Ruiz, A., Quijano, C., Lourenco, C.F., Movilla, N., Enriquez, J.A., Rodriguez-Pascual, F., Rial, E., et al. (2010). Cyclosporine A-induced nitration of tyrosine 34 MnSOD in endothelial cells: role of mitochondrial superoxide. *Cardiovascular research* 87, 356-365.

Tong, W.H., and Rouault, T. (2000). Distinct iron-sulfur cluster assembly complexes exist in the cytosol and mitochondria of human cells. *Embo J* 19, 5692-5700.